The spinal nerve roots

Spinal nerve roots are often subjected to mechanical deformation in various disorders of the spine, ranging from acute spine trauma to degenerative conditions. Nerve root deformation can be related to clinical symptoms such as pain and neurological deficit in back and legs, and is therefore usually referred to the Low-back pain syndrome (LBP), (Nachemson & Andersson 1982). Since compression injury of the spinal nerve roots is an important pathogenic factor in LBP, particularly in sciatica, it may seem surprising that there have been only a few experimental studies on nerve root compression (Gelfan & Tarlov 1956, Sharpless 1975). The results of these studies indicate that spinal nerve roots might be more susceptible to compression injury than the peripheral nerves. However, no critical pressure levels for negative influence of compression on nerve root nutrition or function were determined. Due to anatomical differences, information on the effects of compression on spinal nerve roots can not be directly extrapolated from studies on peripheral nerves (Murphy 1977, Rydevik et al. 1984).

Gross and microscopic anatomy

The nerve roots are the link between the central and the peripheral nervous systems. Anatomically they belong to the central nervous system, but physiologically they are more closely related to the peripheral nervous system. The nerve fibers leave the spinal cord as small rootlets or fila radicularia, which caudally converge into common nerve root trunks. These nerve roots run within the spinal canal and leave it through one of the intervertebral foramina, which are formed by pedicles, articular processes and vertebral bodies of two adjacent vertebrae, including the intervertebral disc (Figure 1). By definition, the dorsal nerve roots end at the dorsal root ganglion. The ventral nerve roots end at a corresponding level (Figure 2).

The axons of the spinal nerve roots are located in the endoneurial space, in which they are surrounded by loose connective tissue called the endoneurium, (Figure 3). There are unmyelinated and myelinated axons in both ventral and dorsal nerve roots. The diameters of the myelinated axons of the human nerve roots range between 1.5 and 16 μm, and the unmyelinated axons range between 0.4 and 1.6 μm (Gamble & Eames 1966). Thomsen observed that the organisation of the nerve root endoneurium is separated into a "central glial segment" and a "peripheral nonglial segment" (Thomsen 1887). The glial segment has a microscopic anatomy that resembles that of the brain, with astrocytes, oligodendrocytes and microglia (Tarlov 1937). The nonglial segment is more similar to a peripheral nerve, but has small islets of neuroglia. The two segments have a "dome-shaped" junction 1–3 mm after the rootlets leave the spinal cord (Tarlov 1937, Berthold et al. 1984). The endoneurium also contains longitudinally oriented collagen fibrils, fibroblasts and blood vessels

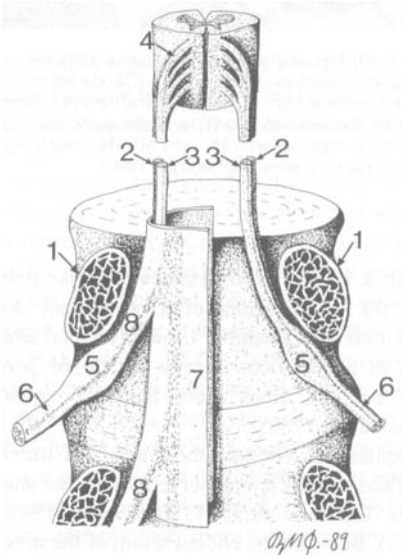

Figure 1. Drawing of the intraspinal course of a human lumbar spinal nerve root segment. The vertebral arches have been removed by cutting the pedicles (1), and the opened spinal canal can be viewed from behind. The ventral (2) and dorsal (3) nerve roots leave the spinal cord as small rootlets (4) that caudally converge into a common nerve root trunk. Just prior to leaving the spinal canal, there is a swelling of the dorsal nerve root called the dorsal root ganglion (5). Caudal to the dorsal root ganglion, the ventral and the dorsal nerve roots mix and form the spinal nerve (6). The spinal dura encloses the nerve roots both as a central cylindrical sac (7), and as separate extensions called root sleeves (8). (Reproduced with permission from, Olmarker K, Thesis, Gothenburg 1990).

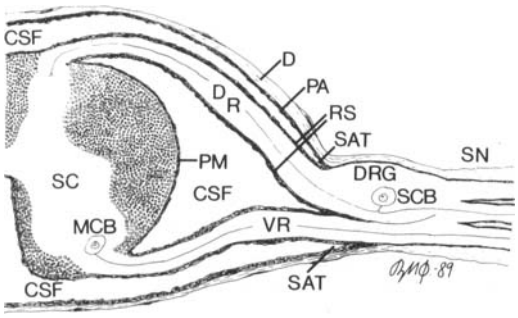

Figure 2. Cross-section of a segment of the spinal cord (SC), a ventral (VR) and a dorsal (DR) spinal nerve root. The cell bodies (MCB) of the motor axons, which run in the ventral nerve root, are located in the anterior horn of the gray matter of the spinal cord. The cell bodies (SCB) of the sensory axons, which run in the dorsal nerve root, are located in the dorsal root ganglion (DRG). The ventral and dorsal nerve roots blend just caudal to the dorsal root ganglion, and form the spinal nerve (SN). The spinal cord is covered with the pia mater (PM). This sheath continues out on the spinal nerve roots as the root sheath (RS). The root sheath reflects to the pia-arachnoid (PA) at the subarachnoid triangle (SAT). Together with the dura (D), the pia-arachnoid forms the spinal dura. The spinal cord and nerve roots are floating freely in the cerebrospinal fluid (CSF) in the subarachnoid space. (Reproduced with permission from, Olmarker K, Thesis, Gothenburg 1990).

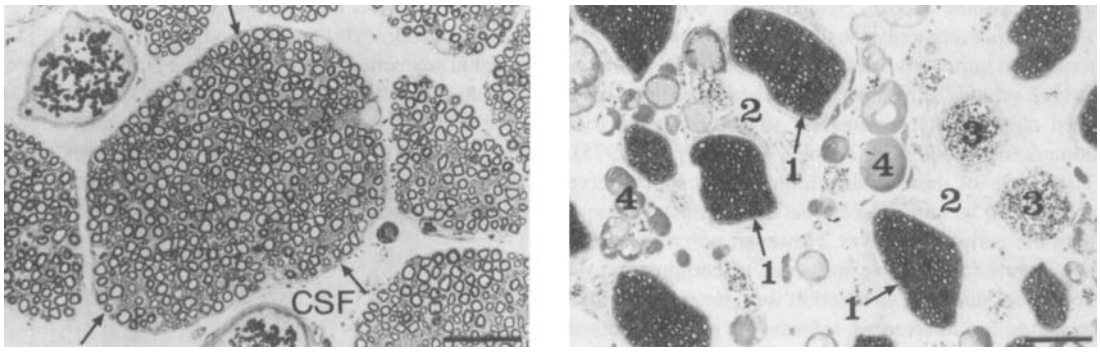

Figure 3. (Left) The axons of the spinal nerve roots are located in the endoneurial space, which is enclosed only by the thin root sheath (arrows) and cerebrospinal fluid (CSF), (Cauda equina from pig, Stain: Richardsson, Bar = 100 μm).
(Right) The endoneurium of the peripheral nerves is similar to that of the nerve roots. In the peripheral nerve, however, the axons are enclosed by the perineurium (1) and the epineurium (2). Blood vessels are located between the different nerve fascicles in the epineurium (3) together with fat cells (4), (N. tibialis from rabbit, Stain: Richardsson, Bar = 100 μm). (Reproduced with permission from, Olmarker K, Thesis, Gothenburg 1990).

(Gamble & Eames 1966). However, unlike peripheral nerves, the endoneurium of a nerve root does not contain mast cells (Gamble 1964). The total amount of protein in nerve roots is only a fifth of peripheral nerves, but six times more than the spinal cord (Stodieck et al. 1986).

The spinal dura encloses the spinal cord, the cerebrospinal fluid and the spinal nerve roots in the shape of a cylinder (Cohen et al. 1991, Rauschning 1983, 1987; Figure 1). Between the endoneurium of the nerve roots and the cerebrospinal fluid there is a structural analogue to the pia of the spinal cord called the root sheath (Waggener & Beggs 1967, McCabe & Low 1969), (Figures 2 and 3). This root sheath is usually formed by 3–4 layers of cells (Haller & Low 1971, Steer 1971). However, as many as 12 layers of cells have been observed in some species (Haller & Low 1971). The cells of the inner layers are similar to the perineurial cells of peripheral nerves. They are joined by desmosomes and are tightly packed together. There is a general agreement that the barrier function of the root sheath is delegated to these cells and their basal membranes (Haller & Low 1971, Steer 1971).

In peripheral nerves, the axons run in a wave-form pattern (Clarke & Bearn 1972, Thomas & Olsson 1984). This may be seen macroscopically as dark and pale bands across the nerve fascicles when observing the nerve trunk in incident light, and have been named "the spiral bands of Fontana". This anatomical feature, which has been suggested to compensate for elongation of the nerve, has not been observed in spinal nerve roots (Sunderland 1978).

Vascular anatomy

The vascular anatomy of the nervous structures of the spinal canal was originally described in the last decades of the nineteenth century (Duret 1873ab, Adamkiewicz

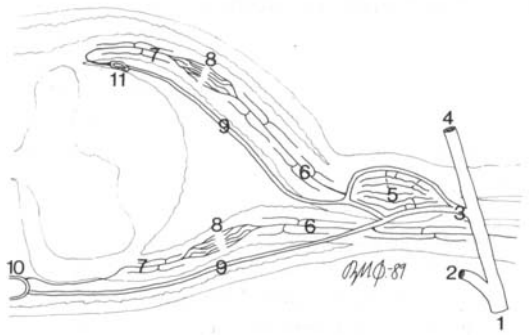

Figure 4. Schematic drawing of vascular supply to the spinal cord and nerve roots. When the intermediate branch of the segmental artery (1) enters the spinal canal it divides into an anterior spinal canal branch (2), a nervous system branch (3), and a posterior spinal canal branch (4). The nervous system branch joins the nerve root and forms a ganglionic plexus (5) and caudal nerve root arteries running in cranial direction (6). From the vaso corona of the spinal cord there are cranial nerve root arteries (7) running in caudal direction. The caudal and the cranial nerve root arteries anastomoze within the cranial half of the nerve root (8). From the nervous system branch there are also medullary feeder arteries (9). These vessels run in cranial direction through the subarachnoid space, without any connections to the nerve root arteries, to the vasa corona of the spinal cord, where 10) is the anterior spinal artery and 11) is one of the two dorsolateral spinal arteries. (Reproduced with permission from, Olmarker K, Thesis, Gothenburg 1990).

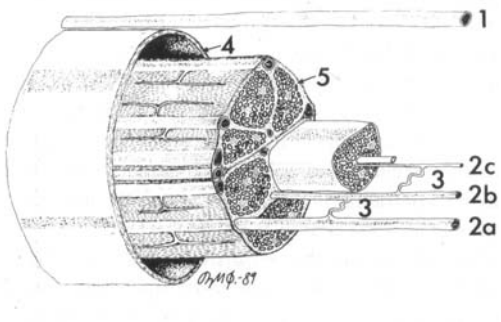

Figure 5. Schematic presentation of some anatomical features of the intrinsic arteries of the spinal nerve roots. The arterioles within the cauda equina may be referred to either the extrinsic (1) or the intrinsic (2) vascular system. From the superficial intrinsic arterioles there are branches that continue almost at right angle down between the fascicles. These vessels often run in a spiraling course, thus forming vascular "coils" (3). When reaching a specific fascicle they branch in a T-like manner, with one branch running cranially and one caudally, forming interfascicular arterioles (2b). From these interfascicular arterioles there are small branches that enter the fascicles where they supply the endoneurial capillary networks (2c). Arterioles of the extrinsic vascular system run outside the spinal dura (4) and have no connections with the intrinsic system by local vascular branches. The superficial intrinsic arterioles (2a) are located within the root sheath (5). (Reproduced with permission from, Olmarker K, Thesis, Gothenburg 1990).

1881, 1882, Kadyi 1886, Tanon 1908). Except for some occasional reports (Suh & Alexander 1939, Herren & Alexander 1939) there was no particular interest in the blood supply of the spinal cord and roots during the first half of this century. However, a rising interest in the capability of the spinal cord to recover from vascular lesions and its reaction to vascular surgery initiated a number of investigations on the collateral circulation of the spinal cord arteries (Adams & van Geertruyden 1956, Fried & Doppman 1958, Gillilan 1958, Corbin 1961, Lazorthes et al. 1966, 1971, Crock & Yoshizawa 1976, Dommisse 1976). There has also been at least two theses on spinal nerve root vascularisation (Desproges-Gotteron 1955, Viraswami 1963). The following presentation will try to provide a summary of the current concept of the vascularisation of the spinal nerve roots of the cauda equina.

The segmental arteries from the aorta and the a. iliaca communis divide into three major branches; i) an anterior branch, which supplies the posterior abdominal wall and the lumbar plexus, ii) a posterior branch, which supplies the paraspinal muscles and facet-joints, and iii) an intermediate branch. The intermediate branch in turn generally divides into three subdivisions; i) anterior spinal branches, which supply the posterior aspects of the vertebral bodies and discs, ii) posterior spinal branches, which supply the vertebral arches, the epidural fat and the spinal dura, and iii) nervous system branches (Crock & Yoshizawa 1976), (Figure 4).

The nervous system branches divide into i) medullary feeder arteries (extrinsic system), which supply the arteries of the spinal cord without giving any branches to the nerve roots they are following along their course through the subarachnoid space, and ii) vessels that incorporate with either of the two nerve roots (intrinsic system; Parke et al. 1981). Thus, the vessels of the extrinsic system do not directly take part in the nutrition of the nerve roots. Embryologically, there are 124 medullary feeder arteries at 31 segmental levels. These arteries are soon reduced in number, and at birth there are only about 8 remaining (Parke et al. 1981). Thus, medullary arteries supply more than one segment of the spinal cord each (Lazorthes et al. 1971).

The vessels that supply the ventral roots form 1–3 caudal radicular arteries that are located within the root sheath and run cranially, towards the spinal cord, and are part of the "intrinsic system" (Figure 5). In the dorsal root, however, the corresponding vessels first form a "ganglionic plexus" around the dorsal root ganglion before they continue cranially as caudal radicular arteries. The caudal radicular arteries of both the ventral and the dorsal roots anastomose with the cranial radicular

arteries, which are derived from the vascular network of the spinal cord, at the cranial half of the nerve roots. Thus, blood flow is supplied from both cranial and caudal directions. At the location where these two vascular networks anastomose, the vasculature of the nerve roots is less developed. It has therefore been suggested that this region of a relative "hypo-vascularisation" may be a particularly vulnerable site of the nerve roots (Parke et al. 1981, Parke & Watanabe 1985).

The arteries of the intrinsic vessels are located mainly in the outer layers of the root sheath. Occasionally they are also found deeper in the nerve root tissue between, or even within the fascicles (Parke & Watanabe 1985). By "T"-like branchings, the arteries provide each fascicle with a number of parallel running interfascicular arterioles (Figure 5). There are arterial coils and vascular loops present that will compensate for elongation of the vessels in both axial direction and between the fascicles (Parke & Watanabe 1985, Petterson & Olsson 1989). Within the fascicles, (ie., in the endoneurial space), the endoneurial capillaries run parallel to the axons.

The venous system has an organisation similar to the arteries. The largest veins, however, do not only course together with the corresponding arteries as in peripheral nerves (Lundborg 1970). Instead they also have a "spiraling" course deeper in the nerve roots (Parke & Watanabe 1985). The veins of the nerve roots also differ from the arteries as they occasionally drain through the spinal dura, out into the epidural venous plexus.

Differences from peripheral nerves

One may summarize some of the morphologic and vascular differences between peripheral nerves and spinal nerve roots as follows:

- The axons of the nerve roots are enclosed by the thin root sheath, cerebrospinal fluid and meninges. The axons of the peripheral nerves are enclosed by the epineurium and the perineurium.
- There is less endoneurial collagen in spinal nerve roots than in peripheral nerves.
- The axons of a peripheral nerve are arranged as the "spiral bands of Fontana". This is not the case for spinal nerve roots.
- There is no fascicular branching in spinal nerve roots, as opposed to in peripheral nerves.
- The arteriolar and venular networks are less developed in spinal nerve roots than in peripheral nerves.
- There is no regional supply to the intrinsic vasculature of spinal nerve roots, unlike in peripheral nerves.
- The intrinsic vessels of the spinal nerve roots are mainly located superficially. In peripheral nerves, the vessels are often found deep in the epineurium, between the fascicles.
- The intrinsic vasculature of spinal nerve roots is formed by two separate networks. One coming from the vasa corona of the spinal cord and one from vessels at the intervertebral foramen. At the region where they anastomose there is an area of "hypovascularity" that may be particularly susceptible to mechanical deformation.

These anatomical characteristics of spinal nerve roots have been suggested to make the spinal nerve roots more susceptible to compression trauma than the peripheral nerves (Murphy 1977, Rydevik et al. 1984, Parke & Watanabe 1985).

Effects of compression

In 1956, Gelfan and Tarlov studied the effects of compression on spinal cord, nerve roots and peripheral nerves (Gelfan & Tarlov 1956). The authors used a compression device that was made of a syringe that, when inflated by a compressed-air system, compressed the nerve tissue between two foam-rubber surfaced metal plates. The study showed that the spinal cord and nerve roots seemed to be less resistant to compression than peripheral nerves. However, the compression device for peripheral nerves was never calibrated and therefore no exact comparison could be made between the effects on spinal nerve roots and peripheral nerves.

Using a fluid-filled balloon with connected pressure transducer, Sharpless compared the effects of compression on conduction properties of peripheral nerves and spinal nerve roots (Sharpless 1975). The study indicated that spinal nerve roots were more sensitive to compression than peripheral nerves and that very low pressures might interfere with the normal impulse conduction of spinal nerve roots.

In conclusion, previous experimental studies indicate that spinal nerve roots seem to be more sensitive to compression than peripheral nerves. However, no critical pressure levels for compression-induced impairment of function or nutrition of the spinal nerve roots were determined.

Compression-induced changes in the porcine cauda equina

Acute compression (Olmarker et al. 1991a)

There are at least three criteria that should be fulfilled by a suitable experimental model of nerve root compression; 1) the nerve roots should be of an adequate length to allow experimental analyses of various parameters, 2) the spinal cord should be absent in the preparation to facilitate neurophysiologic recordings, and 3) it would be preferable to have the site of compression at as low a segmental level as possible to limit any neurologic deficit in a chronic situation. These criteria thus suggest that the cauda equina would be suitable for nerve root studies. Unlike most other readily available experimental animals, the pig was found to have a cauda equina below the level of the mid-sacrum, which showed certain similarities to the human cauda equina.

The pigs were placed prone on an operating table with the hind part of the pig slightly elevated to reduce surgical bleeding. A 10–15 cm long midline incision was made over the sacrum and coccyx. Laminectomies of the 1st and 2nd coccygeal vertebrae were performed. The exposure also included removal of facet-joints and pedicles. To expose the cauda equina, the posterior parts of the epidural membrane were excised and the epidural fat was carefully removed.

The nerve roots were compressed towards the ventral aspect of the spinal canal by an inflatable plastic balloon (diameter 10 mm; Figure 6). The shape of the the spinal canal, including the intervertebral disc, is relatively flat at this level, which thus provides a suitable surface for the nerve root compression. The balloons were made by welding thin and pliable polyethylene sheets into cylinders. One end of these cylinders was sealed with a silk ligature and the other was connected to a polyethylene tube (diameter 1 mm). The balloons were positioned between the nerve roots and a transparent plexiglass plate which was held by two L-shaped pins, and were inflated by a compressed-air system (Stille-Werner, Stockholm, Sweden). This system automatically compensates for any leakage of air, thereby maintaining the pressure at a constant level troughout the experiments (Figure 6). When inflated, the balloons compressed the nerve roots towards the underlying discs and vertebral bodies. The compressed-air system could be set at any pressure level in the range of 0–600 mm Hg. During compression, the cauda equina could be observed through the plexiglass plate. It was thus possible to obtain a visual confirmation that the entire cauda equina was compressed by the balloon.

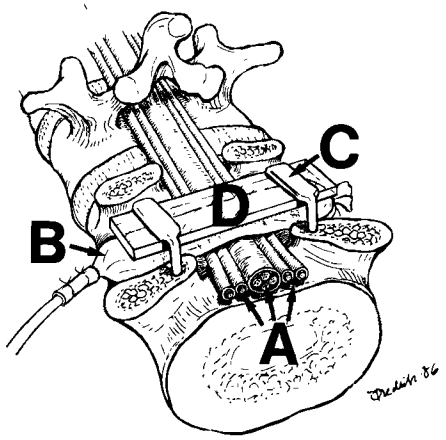

Figure 6. Schematic drawing of experimental model. The cauda equina (A) is compressed by an inflatable balloon (B) that is fixed to the spine by two L-shaped pins (C) and a plexiglass plate (D). (Reproduced with permission from *Spine*, Olmarker et al. 1989b).

The accuracy of pressure transmission from the balloon to the cauda equina was investigated by exchanging the cauda equina with a rabbit abdominal vein. The vein was connected to a compressed-fluid system with an attached manometer (Figure 7). The manometer of this compressed-fluid system was calibrated against the manometer of the compressed-air system which was used to inflate the balloon. The pressure level of the compressed-fluid system was slowly increased, with a known pressure in the balloon. When the first signs of leakage of saline through the vein in the compression zone was observed, the pressure level of the compressed-fluid system was noted. The difference between this pressure and the pressure in the balloon could thus be calculated (Rydevik et al. 1981). Such pressure differences were found to be less than 5 mm Hg at balloon pressure levels in the range of 0–200 mm Hg.

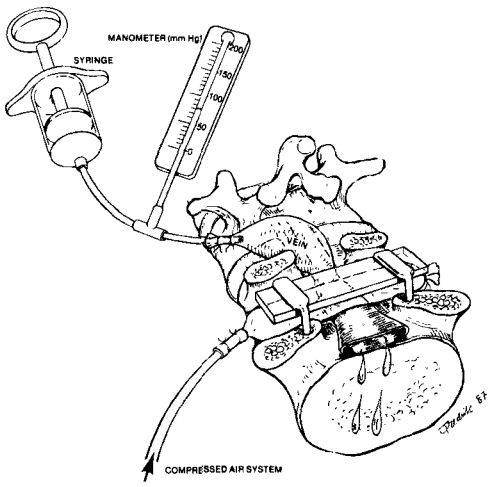

Figure 7. Experimental set-up for testing the accuracy of pressure transmission from the balloon to the nerve roots. For further details, see text. (Reproduced with permission from *Spine*, Olmarker et al. 1989b).

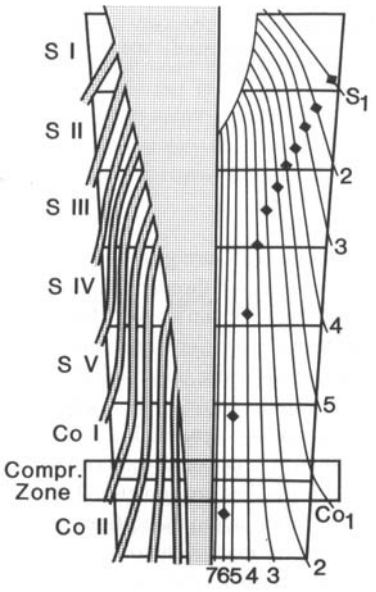

Figure 8. Schematic presentation of the porcine cauda equina at the level of the sacrum and the two upper coccygeal vertebrae. The left half of the drawing demonstrates the spinal dura enclosing the cauda equina, both as a common central sac, and as separate extensions, called root sleeves. In the right half, the location of the dorsal root gangliae (squares), and the intraspinal course of the nerve tissue of the cauda equina are shown. The dorsal root gangliae are mainly located cranial to the compression zone. Roman numerals (left side) indicate vertebral levels, and arabic numerals (right side) indicate nerve root levels. (Reproduced with permission from *Spine*, Olmarker et al. 1991a).

The experimental investigations, as described below, comprized compression at two different onset rates. The balloon was inflated either by starting the compression by flipping the switch with a preset pressure level in the compressed-air system, or by slowly increasing the pressure in the balloon to the desired level during approximately 20 seconds. The first mode of compression onset resulted in a rapid inflation of the balloon, and thus rapid compression of the cauda equina. To determine the rate of this rapid onset of compression, the uninflated and flattened balloon was held between a tracing pen of a Grass 7B Polygraph recorder (Grass Instrument Co., Quincy, Mass.) and a piece of wood. When the balloon was inflated, it thus affected the tracing pen. The movement of the pen was registered on the recording paper, which was running with a known speed. The time from the start of inflation to the point of complete inflation could thus be measured directly on the paper. After 0.05 seconds, there was an inflation to approximately 90% of the intended value. Complete inflation, (i.e. 100% of the intended value), was obtained after approximately 0.1 seconds. The onset time for the rapid onset rate was therefore determined to 0.05–0.1 seconds. This onset rate was found to be constant in the range of 10–200 mm Hg.

To evaluate the gross anatomy of the porcine cauda equina, the spinal canal was opened from the 1st sacral to the 4th coccygeal vertebrae in 5 pigs of body weight ranging between 25–150 kg. The dural sac was opened and the content of the spinal canal was examined with respect to gross anatomy of the cauda equina, both macroscopically and with the use of an operating microscope. Generally, there were no apparent differences in the gross anatomy of the cauda equina between the pigs of the different sizes studied. The spinal cord terminated approximately at the level of the 2nd sacral vertebra (Figure 8). Since the human spinal cord ends at the level of the 1st lumbar vertebra (Rauschning 1983), the conus medullaris is thus located more caudal in the pig than in the human spine. The dorsal root ganglia of the 1st sacral nerve roots were located close to their respective intervertebral foramina. For the lower nerve roots, however, the dorsal root ganglia were successively more cranial to their respective intervertebral foramina. In fact, the dorsal root ganglia of most coccygeal nerve roots were located within the sacrum (Figure 8). However, the dorsal root ganglia for the most caudal nerve roots (Co_6–Co_7) were found caudal to the 2nd coccygeal vertebra (ie., caudal to the compression zone). At the compression site, (ie., the area between the pedicles of the 1st and 2nd coccygeal vertebrae), the first coccygeal "nerve roots" (Co_1) left the spinal canal just

cranial to the disc, and were therefore not compressed by the balloon in this model (Figure 8). A common dural sac, which usually enclosed 3 pairs of "nerve roots" (Co_5–Co_7), was found in the center of the cauda equina. Lateral to the dural sac there were usually 3 pairs of "nerve roots" (Co_2–Co_4) in separate root sleeves. There are thus both "intrathecal" and "extrathecal" nerves (Wall et al. 1991) represented at the compression site.

The spinal nerve roots receive a nutrition contribution not only from the blood vessels but also via direct diffusion from the cerebrospinal fluid (Rydevik et al. 1990a). To be able to draw any conclusions of similarities between the human cauda equina and the pig cauda equina of the present model, it was therefore necessary also to investigate the presence of cerebrospinal fluid, (i.e. the extension of the subarachnoid space), in the compression model. Through a small incision in the dura, a polyethylene catheter was placed into the subarachnoid space in 5 pigs (bodyweight 25–150 kg). A volume of 3–5 ml of India Ink (Pelikan, Hannover, FRG) was injected. Unlike the consistent gross anatomy of the porcine cauda equina, there were apparent differences in the extension of the subarachnoid space between the different sizes of animals investigated (Figure 9). The cauda equina of the smallest animals (20–40 kg) had a subarachnoid space that was present in all nerves all the way down to the point of exit from the spinal canal. However, with increasing animal size, the subarachnoid space in the root sleeves of the most lateral nerves had become gradually sealed (Figure 9). When the ink had been injected in these larger animals, there was an apparent border where the subarachnoid space ended in the root sleeve. However, already after some minutes there was ink detected macroscopically down into the "sealed" space. This "sealing off" phenomenon was not as apparent for more caudal segments of the cauda equina (Figure 9).

Sections, 1 µm thick, were prepared from various levels of the cauda equina in 5 pigs (bodyweight 25–150 kg) and stained with methylene blue and Azur II (Richardsson et al. 1960). The microscopic anatomy of the pig cauda equina was found to be similar to the human cauda equina (Gamble & Eames 1966, Cohen et al. 1991). The endoneurial space was comprised of a mixture of myelinated and unmyelinated axons, and was separated from the cerebrospinal fluid only by the thin root sheath (Figures 10a–d). However, unlike the human lumbo-sacral dorsal root gangliae, the dorsal root gangliae of the compressed nerves were floating freely in the cerebrospinal fluid (Figure 9 and 10b). At the extrathecal parts of the cauda equina, the root sleeves gradually approached the nerve components,

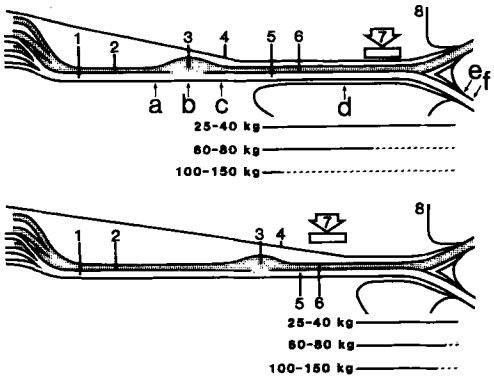

Figure 9. Schematic drawings of the anatomy at the 2nd coccygeal (top) and at the 5th coccygeal nerve root (bottom) level. The ventral (1) and the dorsal (2) nerve roots leave the spinal cord and run in the subarachnoid space surrounded by the cerebrospinal fluid. At the level of the dorsal root ganglion (3) the fibers of the two nerve roots are mixed, and the ventral ramus (5) and dorsal ramus (6) of the spinal nerve is formed. The dura (4) encloses the nerve components until the point where they leave the spinal canal, and where also the epidural membrane (8) approaches the nerve tissue. The compression site (7) is located caudal to the dorsal root ganglion. The 2nd coccygeal nerve roots (top) are the largest nerve roots compressed at their extrathecal course, and the 5th coccygeal nerve roots (bottom) are the largest nerve roots compressed at their intrathecal course, in the presented model.

The extension of the subarachnoid space for the three different sizes of pigs was investigated at both nerve root levels. The results are schematically shown under each drawing. The interrupted lines indicate nerve root segments where there was no intrathecally injected ink present immediately after the injection.

The letters a–f in the upper figure refer to the microscopic cross-sections presented in Figure 10. (Reproduced with permission from *Spine*, Olmarker et al. 1991a).

(Figure 10d). This also resulted in a subsequent reduction of the subarachnoid space. At the last 5–10 mm cranial to the point of exit from the spinal canal, there was a gradual formation of fascicles within the endoneurial space (Figure 10e). Outside the spinal canal, the microscopic anatomy of the nerve tissue changed to that of a peripheral nerve, with an epineurium and a perineurium instead of a root sleeve, and with separate fascicles (Figure 10f). The light microscopic examination also revealed that the major vessels of the intrinsic system of the cauda equina (i.e., arterioles and venules) were found outside the endoneurial space, and were enclosed by the root sheath (Figure 10a). Within the endoneurial space, there were only capillaries present.

To visualize the anatomy of the nerve root vessels, India Ink was infused under pressure in 5 pigs (bodyweight 25–150 kg). The cauda equina was clarified with a modified Spalteholz technique. For comparative reasons, a part of the sciatic nerve at the

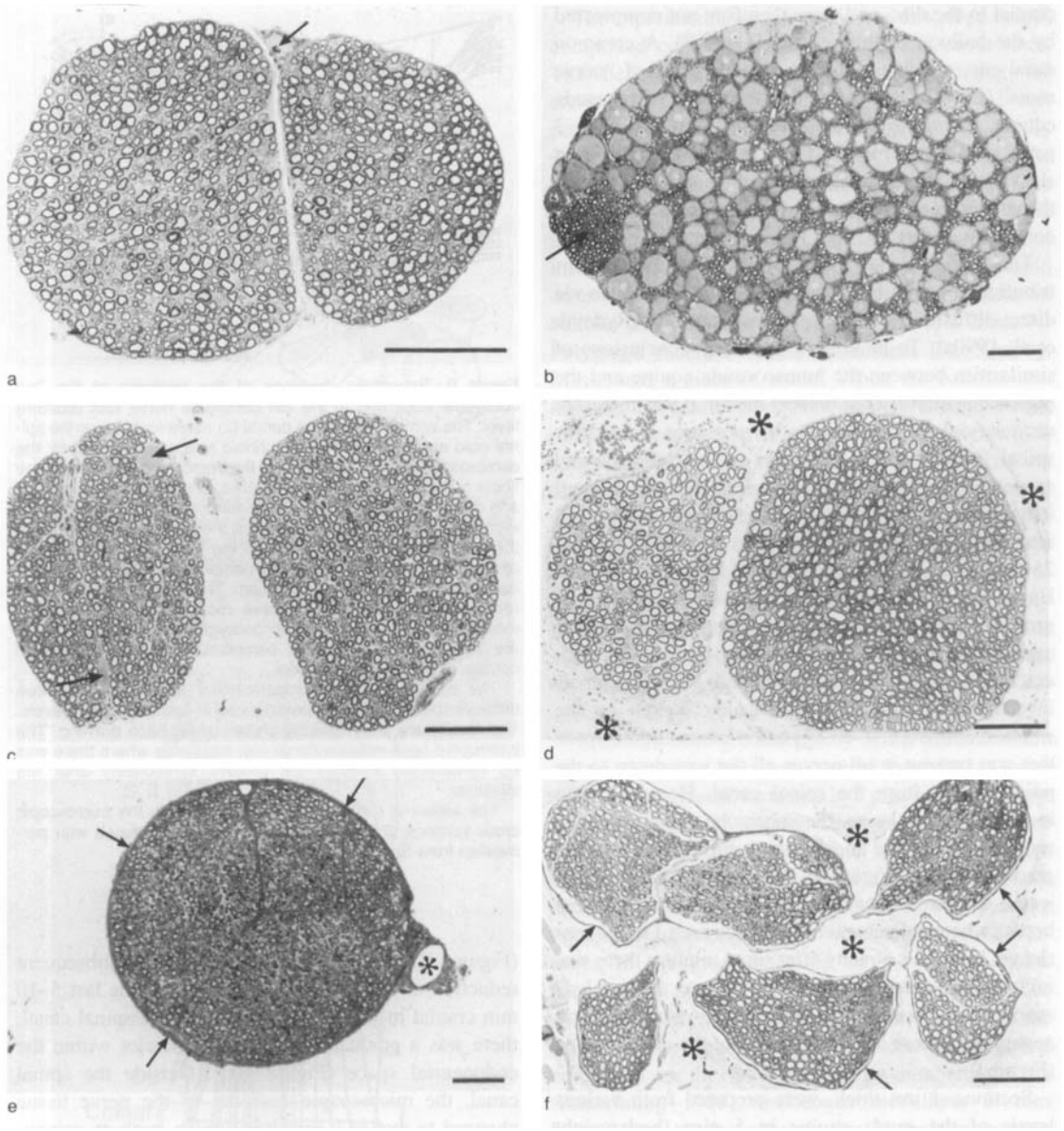

Figure 10. Photographs of microscopic cross-sections from a 2nd coccygeal nerve root pair, (see Figure 9 for orientation).

a) The ventral (right) and the dorsal nerve root just cranial to the dorsal root ganglion. An intrinsic vessel is seen within the root sheath, (arrow).

b) The nerve roots at the level of the dorsal root ganglion. A large number of ganglion cells may be seen in the picture. At this level, the axons of the roots are mixed and form the ventral and the dorsal ramus of the spinal nerve. There is only a minor part of the former ventral root that can be identified, (arrow).

c) The ventral (right) and dorsal ramus of the spinal nerve just caudal to the dorsal root ganglion. Some of the most caudal ganglion cells may be seen in the dorsal ramus, (arrows).

d) At the extrathecal course of the ventral ramus (left) and dorsal ramus of the spinal nerve, they are enclosed by an extension of the spinal dura called the root sleeve, (asterisks).

e) The ventral ramus of the spinal nerve just prior to leaving the spinal canal. The root sleeve (arrows) has now approached the nerve tissue. There is no longer a subarachnoid space present between the nerve tissue and the root sleeve. Also note the formation of a fascicular pattern within the nerve tissue. Outside the root sleeve is a cross-cut extrinsic arteriole (asterisk).

f) The ventral ramus of the spinal nerve just outside the spinal canal. The different fascicles have separated, and are enclosed by epineurial tissue (asterisks), and by a perineurium (arrows). Extra-fascicular vessels may be found between the fascicles in the epineurium, (Bar = 100 μm in all pictures). (Reproduced with permission from *Spine,* Olmarker et al. 1991a).

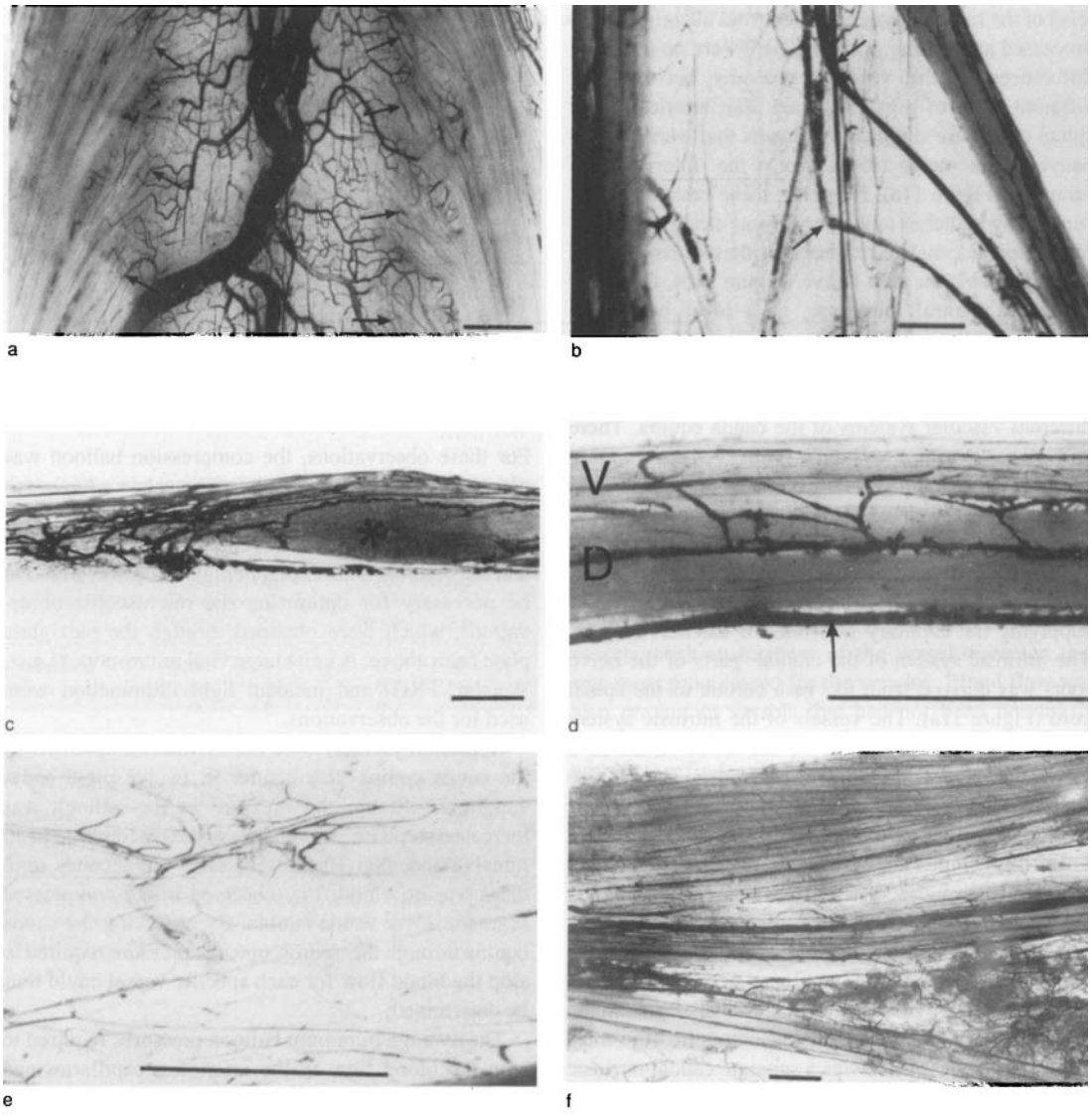

Figure 11. Photographs of ink-injected and clarified specimens of the porcine cauda equina.

a) The ventral aspect of the segment of the spinal cord from which the 2nd coccygeal nerve roots leave. The anterior spinal artery in the center is supplied with blood from an ascending medullary feeder artery coming from the lower left corner. Vessels from the vasa corona of the spinal cord are joining the nerve roots when they leave the spinal cord (arrows).

b) The picture shows the cauda equina in the central dural sac to the left and a nerve root pair that has passed through the dural sac and is now enclosed by its root sleeve to the right. Two extrinsic vessels that are running together with the nerve root pair are passing through the dural sac more caudal than the nerve roots (arrows). These vessels are also providing the meninges with small branches.

c) The dorsal root ganglion (2nd coccygeal) demonstrates a capillary-dense area of the nerve roots, (asterisk). The intrinsic vessels demonstrate a coiling or tortuous course. There are branches from the intrinsic vessels out into the epidural fat, (arrows). (Cranial side to the right in the picture).

d) Vascularisation of the ventral (V) and dorsal (D) ramus of the right 2nd coccygeal spinal nerve. From a central intrinsic vessel of the dorsal ramus there are "T-like" branches that supply the ventral ramus as well. There is also an extrinsic vessel seen in the picture, with no visible branches to the intrinsic vasculature of the nerve tissue, (arrow).

e) Blood vessels within the spinal dura.

f) Vascularisation of a part of the right sciatic nerve at the level of the hip joint. Note the well developed vascular network, with numerous branches between fascicles and surrounding fat, (Bar = 1 mm in all pictures). (Reproduced with permission from *Spine,* Olmarker et al. 1991a).

level of the hip joint was collected from all animals and processed in a similar manner. There were no observed differences in the vascular anatomy between the different sizes of pigs examined. The arteries of the spinal cord were supplied by vessels that were accompanying the nerve roots from the intervertebral foramina (Figure 11a). However, these vessels did not supply any branches to the nerve roots along the course in the spinal canal. Extrathecally, these vessels were located outside the root sleeve (Figure 11b). Upon entering the central dural sac, at a level below the entrance of the corresponding nerve root pair, they supplied the meninges with small branches (Figure 11b and e). It was thus apparent that there were two different vascular systems of the cauda equina. There was one "extrinsic system", with vessels running between the segmental arteries outside the spinal canal and the vasa corona of the spinal cord, which did not directly participate in the nutrition of the nerve tissue. There was also one "intrinsic system" of vessels which were running within the root sheath, and which were supplying the capillary networks of the nerve tissue. The intrinsic system of the cranial parts of the nerve roots was derived from the vasa corona of the spinal cord (Figure 11a). The vessels of the intrinsic system were found to run parallel to the nerve fibers in a straight course within the nerve roots. There were frequent vascular loops and also a "coiling" or "tortuous" course of these vessels (Figure 11c and d). From the venules and arterioles, the branches left at almost right angles. These branches either supplied superficially located and longitudinally running vessels of lesser caliber, or penetrated between the axons to supply the endoneurial capillary networks (Figure 11d). It was not evident if the intrinsic vessels from the cranial part of the nerve roots also supplied the most caudal parts, or if there was a separate caudal intrinsic system of vessels. Indeed, there were connections between extraspinal vessels and the most caudal intrinsic vessels detected at the intervertebral foramen. However, a region of "relative hypovascularity" in an anastomosing region between the two vascular systems, similar to that described by Parke and collaborators, could not be detected (Parke et al. 1981). Generally, the arteriolar and venular vasculature of the cauda equina was less developed than that of the peripheral nerves (Figure 11f). Although there was no regional supply of arteriolar blood to the intrinsic vascular system of the nerve roots, there were regional connections between the venules of the intrinsic system and venules in the surrounding epidural fat observed, (Figure 11c). Within the central dural sac there were also interradicular vessels that connected the vascular networks of different nerve roots.

Table 1. Average minimum balloon pressures (BP; mm Hg) required to stop the flow in the arterioles, capillaries and venules

BP	n	$\bar{x}$	*SD*
Arterioles	11[a]	127	*18*
Capillaries	12	40	*6*
Venules	12	30	*10*

[a]No arterioles could be identified in one of the pigs.
Reproduced with permission from *J Orthop Res*, Olmarker et al. 1989a.

Blood flow (Olmarker et al. 1989a)

For these observations, the compression balloon was placed under the cauda equina. The cauda equina was thus compressed dorsally, between the plexiglass plate and the balloon, instead of ventrally, between the disc and the balloon. This experimental set-up was found to be necessary for optimising the microscopic observations, which were obtained through the plexiglass plate from above. A Leitz large vital microscope (Leitz, Wetzlar, FRG) and incident light illumination were used for the observations.

Occlusion pressures for the various components of the cauda equina vasculature. In twelve pigs, bodyweight 25–40 kg, the pressure in the balloon was increased stepwise, 5 mm Hg every 20 seconds up to 50 mm Hg and then 10 mm Hg every 20 seconds until there was no blood flow observed in the compressed segment of the cauda equina. By observing the cauda equina through the microscope, the pressure required to stop the blood flow for each specific vessel could thus be determined.

The average minimum balloon pressures required to stop the blood flow in the arterioles, capillaries and venules are presented in Table 1. When the pressure in the balloon was increased, a gradually diminishing diameter of the vessels could be observed through the microscope. This effect was first seen 10–50 mm Hg below the pressure level required to stop the blood flow in that specific vessel. As a further sign of an impaired flow, the arterioles started to pulsate at a pressure level approximately 30–40 mm Hg below the occlusion pressure. A corresponding phenomenon could not be observed for the capillaries or the venules. Generally, the capillary blood flow seemed to be dependent upon the flow in the connected venules. Thus, when the flow in an adjacent venule was impaired, there were often signs of an impaired flow in the connected capillary networks.

The correlation between the pressure required to stop the blood flow in the different vessels and the mean

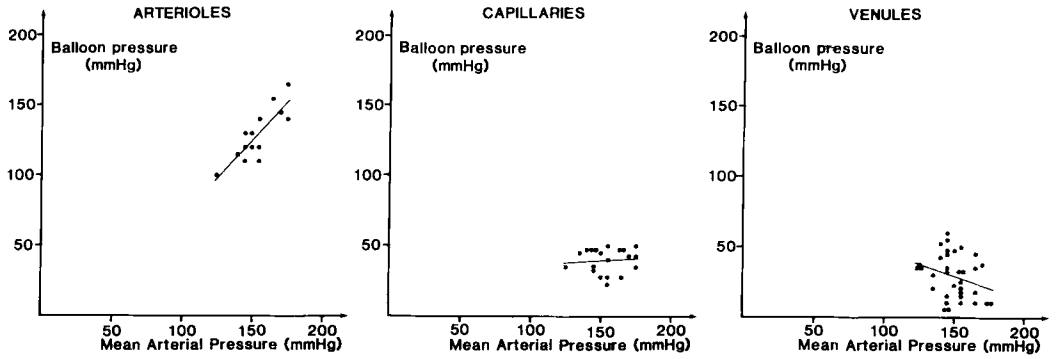

Figure 12. Diagrams showing correlation between mean arterial pressure and the pressure required to stop blood flow in arterioles, capillaries, and venules. (Reproduced with permission from *J Orthop Res,* Olmarker et al. 1989a).

Table 2. Effects of compression on recirculation. The results from twelve animals, three for each subseries, are graded on a three grade scale

	50 mm Hg		200 mm Hg	
	10 min	2 h	10 min	2 h
Initial flow	0	(+)	0	0
	0	0	0	(+)
	0	0	0	0
Hyperemia	+	+	+	+
	+	+	+	+
	+	+	+	+
Edema	0	+	0	+
	0	+	0	+
	0	+	0	+

0 no changes, (+) moderate changes, and + marked changes. Reproduced with permission from *J Orthop Res,* Olmarker et al. 1989a.

arterial pressure was statistically significant ($p < 0.001$) for the arterioles (r = 0.83), but not for the capillaries (r = 0.09) or for the venules (r = –0.28; Figure 12).

Recirculation of the cauda equina vasculature following compression for various times and at various levels. The nerve roots were exposed to compression at 50 mm Hg for 10 minutes or 2 hours, or at 200 mm Hg for 10 minutes or 2 hours. The recirculation of the cauda equina was analysed regarding: initial flow (ie., immediate versus delayed recirculation), hyperemia (i.e., normal versus increased blood flow) and intraneural edema formation (i.e., normal versus increasing opacity of nerve root tissue with increasing difficulties to focus on vessels). When compression was ended, initial flow, hyperemia and edema formation were estimated according to a three grade scale (Table 2). Recirculation was observed immediately except in two animals where there was initially a reduced flow in some of the venules. However, in these animals the flow was completely restored within 1 minute. In all animals there was evidence of a hyperemia, as compared to before beginning the compression in this series. The hyperemia was seen as a dilatation of the vessels, with an increase of the vessel diameter, that was most pronounced for the venules. Blood flow was also present in vessels that had not been previously seen in the preparation. The hyperemia developed within the first minute of circulation and gradually decreased after 5–10 minutes. Intraneural edema was seen as an increasing opacity of the nerve roots in the microscope and difficulties in getting a sharp image of the intrinsic vessels. The edema developed within the first 10 minutes of recirculation, but was only seen in nerve roots exposed to compression of either 50 or 200 mm Hg for 2 hours.

Nutritional supply (Olmarker et al. 1990a)

The effects of surgical exposure (control = the spinal canal was opened but the compression device was not applied), sham-compression (the compression device was applied but with no inflation of the balloon) and compression at 10 mm Hg, 50 mm Hg, or 200 mm Hg at either the rapid or the slow onset rate, (n = 6 for each of the six subseries) were studied in 48 pigs, bodyweight 25–40 kg. The spinal nerve roots were exposed to control conditions, sham-compression, or compression for a total of 30 minutes. After 25 of these 30 minutes, 0.5 mCi/kg bodyweight of 3-0-methyl-D-glucose-1-^{3}H (Radiochemical Centre, Amersham, England) was injected into v cava superior. The methyl glucose was thus allowed to circulate for the last 5 minutes of the compression period. After the 30

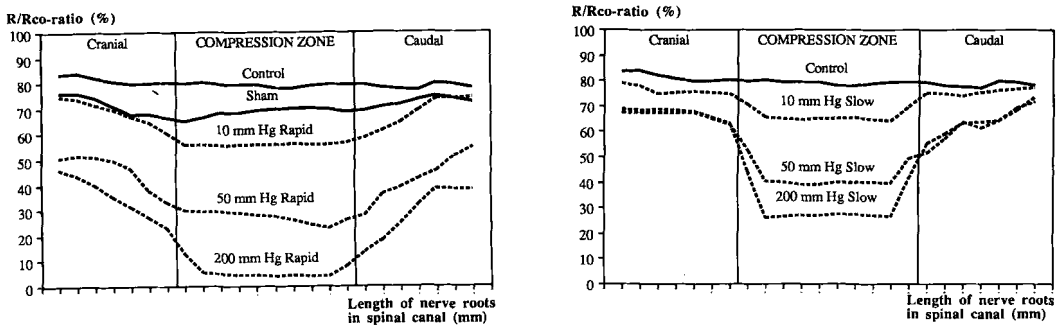

Figure 13. Average R/Rco-ratio for control, sham-compression and compression at the rapid onset rate (left), and control and the slow onset rate (right). (Reproduced with permission from *J Spin Dis*, Olmarker et al. 1990a).

minutes of compression, the entire preparation was frozen with liquid nitrogen, without releasing the compression.

The cauda equina was cut transversely into approximately 1 mm sections, which were analysed in a ß-scintillation counter (Packard Instruments, Stockholm, Sweden). This procedure allowed for calculation of the ratio (R/Rco) between nerve concentration (R) of methyl glucose and blood concentration (Rco) of methyl glusoce in each specimen. The average R/Rco-graphs (i.e., the ratio between the obtained radioactivity in the digested specimen (R) and the radioactivity in the normalized blood (Rco)) for each sub-series were plotted in a diagram with the length of the nerve roots on the X-axis and the R/Rco-ratio on the Y-axis (Figure 13).

Sham-compression was found to induce a statistically significant reduction of the transport of methyl glucose to the compression-zone ($p < 0.01$) as compared with control (Wilcoxon's rank sum test; Figure 13, Table 3). There was a reduction of the transport of methyl glucose to the compressed part of the nerve roots that was proportional to the applied pressure level (Figure 13, Table 3). However, the reduction was more pronounced with rapid onset of compression than with slow onset of compression at corresponding pressure levels. These differences were found to be statistically significant ($p < 0.01$) at all three pressure levels tested (i.e., *10*, *50*, and *200* mm Hg). Outside the compression-zone the average R/Rco-ratio at the slow onset of compression generally approached the control levels more rapidly than with rapid onset of compression. The R/Rco-graphs at the slow onset rate also indicated that there was a reduction of the baselines outside the compression zone that was directly proportional to the compression pressure level.

Table 3. The average R/Rco-ratio within the compression zone of the different subseries are presented, as well as the reduction of these average values as compared to the control series

Experimental series	Average R/Rco-ratio (%)	*SD*	Reduction from control (%)
Control	79	*3*	...
Sham	68	*5*	14
Slow onset of compression			
10 mm Hg	65	*2*	18
50 mm Hg	40	*2*	49
200 mm Hg	27	*5*	66
Rapid onset of compression			
10 mm Hg	56	*4*	29
50 mm Hg	27	*10*	66
200 mm Hg	4	*2*	95

Reproduced with permission from *J Spin Dis*, Olmarker et al. 1990a.

Intraneural edema formation (Olmarker et al. 1989b)

The effects of sham-compression and compression at rapid and slow onset rate and at different durations and pressure levels were studied in 39 pigs, boyweight 25–60 kg, (n = 3 in each subseries). After the compression was released, the pigs received an intravenous injection of 5 ml/kg bodyweight of a filtered preparation of Evans Blue labelled albumin (EBA) that was allowed to circulate for 30 minutes. Frozen longitudinal sections of the cauda equina were analysed by fluorescence-microscopy. The distribution of the EBA complex could be determined as it emits a bright red fluorescence, which contrasts clearly to the green autofluorescence of the nerve tissue. Microvascular permeability, (i.e., the distribution of EBA-complex

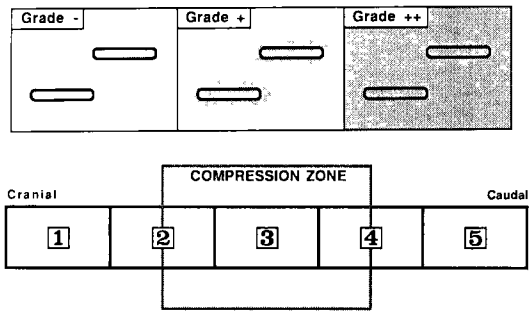

Figure 14. (Top) Schematic drawing of longitudinal sections of three nerve root segments with different degrees of intraneural edema. Each nerve root contains two intraneural capillaries. The distribution of Evans Blue labelled albumin (EBA), within the nerve root in the microscopic sections was graded on a three grade scale; - = EBA only within the vessel lumen (no edema), + = EBA also between the axons in the endoneurial space but only adjacent to the vessels (slight edema), and ++ = EBA between the axons and reaching from one lateral border of the nerve root to the other (pronounced edema). (Bottom) The formation of intraneural edema was studied at 5 different locations of the cauda equina; 1) cranial to the cranial edge zone, 2) at the cranial edge zone, 3) at the center of compression zone, 4) at the caudal edge zone and 5) caudal to the caudal edge zone. (Reproduced with permission from *Spine*, Olmarker et al. 1989b)

within the endoneurial space), was studied at 5 different locations of the cauda equina, regarding degree of edema and fraction of nerve roots involved (Figure 14).

In the sham-compression series there was no EBA detected outside the vessels in the microscopical sections. The edema was more pronounced following rapid onset compression at either 2 hours or 10 minutes of compression than after 2 minutes at both 50 mm Hg and 200 mm Hg compression (Table 4). However, the magnitude and distribution of the edema at the five observation sites was similar for the two pressure levels at corresponding compression durations. The duration of compression thus seems to be more important than the pressure level for the degree of edema formation at compression up to 200 mm Hg. The edema was most pronounced at the edge-zones, but was also observed at the center of the compression zone following the two longer compression times at both compression levels. Generally, the edema formation was not as pronounced for the slow as for the rapid onset rate for the corresponding compression times and pressure levels (Table 5). There was no edema following compression at 50 mm Hg for 2 or 10 minutes. Compression at 50

Table 4. Intraneural edema formation following rapid onset of compression. The degree of edema and fraction of nerve roots involved were studied at 5 different locations of the nerve roots.

Compression	Degree of intraneural edema[a]					Fraction of nerve roots involved[b]				
	1	2	3	4	5	1	2	3	4	5
50 mm Hg										
2 min	-	+	-	++	-	-	+	-	+	-
	-	-	-	+	-	-	+	-	+	-
	-	-	-	++	-	-	-	-	++	-
10 min	-	+	+	+	-	-	++	+	+	-
	-	++	++	+	-	-	+	+	++	-
	-	+	+	++	-	-	+	+	+	-
2 h	-	++	+	++	-	-	+	+	+	-
	-	+	+	++	-	-	+	+	++	-
	-	++	+	++	-	-	+	+	++	-
200 mm Hg										
2 min	-	+	-	-	-	-	+	-	-	-
	-	++	-	+	-	-	+	-	+	-
	-	++	-	++	-	-	+	-	+	-
10 min	-	++	++	++	-	-	++	+	+	-
	-	++	+	++	-	-	+	+	+	-
	-	+	+	+	-	-	+	+	+	-
2 hrs	-	++	+	+	-	-	++	+	+	-
	-	+	+	++	-	-	+	+	++	-
	-	++	+	++	-	-	++	+	++	-

[a]Grading as in Figure 14.
[b]- no nerve roots, + less than 50% of nerve roots, ++ more than 50% of nerve roots.
Reproduced with permission from *Spine*, Olmarker et al. 1989b.

Table 5. Intraneural edema formation following slow onset of compression. The degree of edema and fraction of nerve roots involved were studied at 5 different locations of the nerve roots.

Compression	Degree of intraneural edema[a]					Fraction of nerve roots involved[b]				
	1	2	3	4	5	1	2	3	4	5
50 mm Hg										
2 min	-	-	-	-	-	-	-	-	-	-
	-	-	-	-	-	-	-	-	-	-
	-	-	-	-	-	-	-	-	-	-
10 min	-	-	-	-	-	-	-	-	-	-
	-	-	-	-	-	-	-	-	-	-
	-	-	-	-	-	-	-	-	-	-
2 hrs	-	+	-	+	-	-	+	-	+	-
	-	+	-	+	-	-	+	-	+	-
	-	+	-	++	-	-	+	-	+	-
200 mm Hg										
2 min	-	-	-	++	-	-	-	-	+	-
	-	-	-	+	-	-	-	-	+	-
	-	-	-	+	-	-	-	-	+	-
10 min	-	+	-	++	-	-	+	-	+	-
	-	+	-	+	-	-	+	-	+	-
	-	+	-	+	-	-	+	-	+	-
2 hrs	-	+	+	++	-	-	+	+	++	-
	-	++	++	++	-	-	++	++	++	-
	-	++	++	++	-	-	++	+	++	-

[a and b]See Table 4.
Reproduced with permission from *Spine*, Olmarker et al. 1989b.

mm Hg for 2 hours only induced edema at the edges of the compression zone and not at the center. Following compression at 200 mm Hg for 2 minutes there was edema only at the caudal edge of the compression zone. After 10 minutes of compression the edema was present at both edges. The results for compression at 200 mm Hg for 2 hours were, however, similar to the results for the corresponding pressure level and time for rapid onset of compression.

Impulse propagation (Olmarker et al. 1990b)

Two AO cortical screws were fixed in the lamina of the 5th sacral vertebra and served as stimulating electrodes. Muscle action potentials (MAP) were recorded by two platinum needle electrodes placed into the muscles in the tail and visualized on an oscilloscope. This procedure is reproducible and represents a measurement of the function of the motor nerve fibers of the nerve roots. Nerve function was registered as the amplitude of the first peak of the MAP-recording, and was measured directly on the oscilloscope. This peak reflects the fastest conducting fibers, which also are the fibers with the largest diameter (Gasser & Erlanger 1929). Large diameter fibers are known to be more susceptible to compression (Gasser & Erlanger 1929) and may also be subjected to greater deformation than small diameter nerve fibers (MacGregor et al. 1975). Therefore, analysis of the first peak of the MAP represents a sensitive method for studying changes in the motor fiber propagation in the nerve roots. It has been noted that changes in amplitude of the first peak of the MAP are seen earlier than changes in conduction velocity (Pedowitz et al. 1991, Rydevik et al. 1991a). The present study therefore focused only on changes in MAP-amplitude. Intermittent recordings of MAP's were performed using supramaximal stimulation strength until temperature and amplitude of the MAP's had been constant for 15 minutes. This value of the MAP-amplitude served as baseline (100%) and all recordings during the experiment were expressed in percent of this value. The pressure levels used were; 0 mm Hg (sham, n = 2), 50, 100, and 200 mm Hg. Except for sham-compression, there were 5 animals with the rapid onset and 5 with the slow onset of compression for each pressure level. The nerve roots were compressed for 2 hours and allowed to recover for 1.5 hours, with the compression balloon removed. MAP-recordings were performed 5, 10 and 15 minutes after compression onset, and then every 15 minutes.

The amplitude of the MAP-recordings obtained by intermittent stimulation caudal to the compression

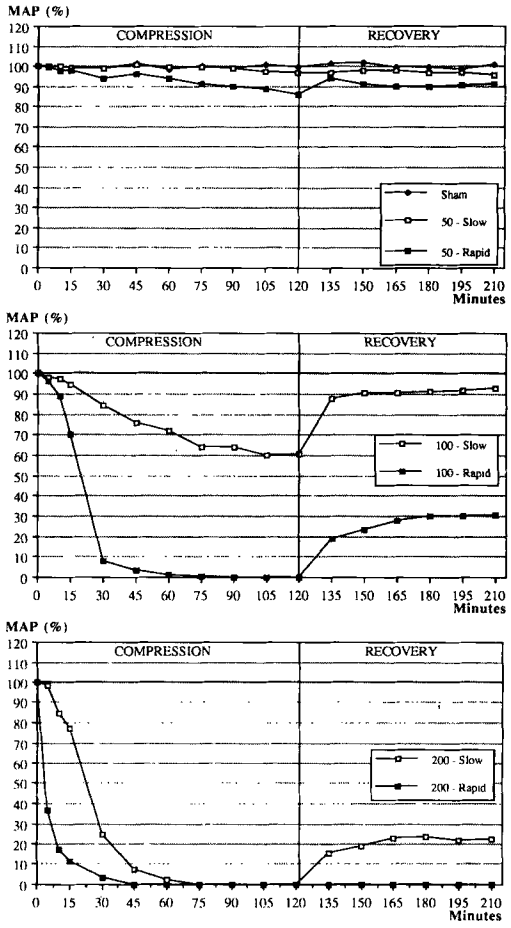

Figure 15. Average amplitude of MAP (muscle action potential), representing conduction of the fastest conducting motor nerve fibers, expressed in percent of baseline value. The diagrams show the results of 2 hours of compression and 1.5 hours of recovery for sham-compression and for rapid and slow onset of compression at 50 mm Hg, 100 mm Hg and 200 mm Hg. (Reproduced with permission from *Spine*, Olmarker et al. 1990b).

zone were always within 5% of the baseline value, which indicates stability of experimental conditions and caudal neuromuscular function. There was no reduction of MAP-amplitudes for sham-compression or for compression at 50 mm Hg with the slow onset rate (Figure 15, Table 6). Compression at 50 mm Hg with the rapid onset rate induced a slight reduction of the MAP-amplitude (Figure 15). This reduction was not significant as compared to slow onset rate or control, using Wilcoxon's rank sum test. Compression at 100 and 200 mm Hg induced reductions in MAP-amplitude that were directly proportional to the applied

Table 6. Average reduction of MAP-amplitude from initial value after 2 hours of compression

Experimental series	Reduction	
	(%)	*SD*
Sham-compression	0.3	*0.7*
Slow onset of compression		
50 mm Hg	1	*2*
100 mm Hg	25	*13*
200 mm Hg	69	*5*
Rapid onset of compression		
50 mm Hg	7	*8*
100 mm Hg	79	*6*
200 mm Hg	93	*5*

Reproduced with permission from *Spine*, Olmarker et al. 1990b.

pressure (Figure 15, Table 6). However, the reduction after rapid onset was generally more pronounced than after slow onset of compression. For these two pressure levels the differences between the two onset rates were found to be statistically significant ($p < 0.01$), at corresponding compression levels. The MAP-amplitude recovered to close to baseline after compression at 100 mm Hg with the slow onset rate. However, after both 100 mm Hg with the rapid and 200 mm Hg with the slow onset rate of compression there was an incomplete recovery of the MAP-amplitude (Figure 15). Following rapid onset of compression at 200 mm Hg there was no recovery in any of the experiments (Figure 15).

General discussion

Experimental model for compression of the porcine cauda equina

The normal neural and vascular anatomy of the porcine cauda equina was found to be similar to that of the human cauda equina. However, there were two anatomical features which will be discussed specifically.

First, with increasing age and bodyweight there was a sealing of the subarachnoid space that started from the caudal end of the nerve roots. This phenomenon was not observed in pigs below 40 kg bodyweight. It was recently observed that diffusion of nutrients from the cerebrospinal fluid may be an important nutritional pathway for the nerve roots (Rydevik et al. 1990a). To mimic the anatomy of the human cauda equina, it may therefore advisable only to use pigs up to 40 kg bodyweight.

Second, the dorsal root gangliae of the compressed nerve roots were located cranial to the compression zone. By definition, the compressed segments of the nerve roots should therefore be termed "spinal nerves" instead of nerve roots. Fontana's spiral bands were also found to be present at the most caudal parts of some nerve roots. The question therefore arises whether the compressed parts of the nerve roots were morphologically more similar to peripheral nerves than spinal nerve roots.

The nerve roots are generaly considered to be the part of the nervous system that run between the spinal cord and the dorsal root ganglion, or a corresponding level for the ventral roots. However, the difference in compression susceptibility between spinal nerve roots and peripheral nerves has been suggested to be based on differences in the surrounding connective tissue layers (Murphy 1977, Rydevik et al. 1984). A more relevant "pathophysiologic" description of the spinal nerve roots would thus be; the part of the nervous system that runs from the spinal cord and is enclosed only by the root sheath, cerebrospinal fluid and meninges. According to the present investigation, this description would be applicable to all parts of the cauda equina compressed by the balloon. The microscopic anatomy typical of a peripheral nerve was found to be present only outside the spinal canal (Figure 10f).

The vascular anatomy of the porcine cauda equina was found to have a close resemblance to the human cauda equina. There was an intrinsic system of vessels that was located within the root sheath and comprised arterioles and venules that supplied the endoneurial capillary networks. There was also an extrinsic vascular system. Unlike the intrinsic system these vessels did not directly participate in the nerve root nutrition by any vascular branches to the intrinsic arterioles along the course of the nerve roots. This observation was in agreement with previous studies on the vascularisation of the human cauda equina (Parke et al. 1981, Parke & Watanabe 1985). However, unlike the findings of Parke and collaborators on the human cauda equina, Petterson and Olsson (1989) recently observed occasional direct branches between the extrinsic and the intrinsic systems in cervical spinal nerve roots of rats.

There is an apparent difference in the vascular anatomy between the peripheral nerves and the nerve roots that may be of importance for differences in susceptibility to compression injury between these tissues. The effects of compression on nerve tissue at pressure levels below 200 mm Hg have been suggested to be based mainly on an impairment of the nutrition, rather than direct mechanical injury to the axons (Dahlin et al. 1986). However, the peripheral nerves have a much more developed network of arterioles and venules than the nerve roots (Figures 11d and f). Also, the main vessels of the cauda equina are always located superficially and might therefore easily be exposed to mechanical deformation (Figures 10a). Conversely, the vessels of the peripheral nerves may be found between the fascicles, in the epineurium, and may thereby be better protected from mechanical deformation (Figure 11f). This hypothesis is supported by the present investigations which indicate that the pressure required to induce vascular stasis is lower for nerve roots (Olmarker et al. 1989a, 1990a) than for peripheral nerves (Rydevik et al. 1981), particularly on the venular side.

As opposed to the peripheral nerves, the nerve roots have no regional arteriolar blood supply. This might be particularly important in situations with compression at more than one site. The vascular anatomy of the porcine cauda equina as described, demonstrates all features that are characteristic of the vasculature of human spinal nerve roots (Parke & Watanabe 1985).

The presented model showed both a well-controlled pressure transmission and a close resemblance of neural and vascular anatomy to the human cauda

equina. The easy surgical approach of the porcine cauda equina and the sufficient length of the nerve roots offer unique features for experimental studies on nerve roots. The present model allows for reproducible, pressure-induced changes in nerve root pathophysiology. The porcine cauda equina may also be particularly suitable for chronic compression studies, since neurological deficits would be localized only to the tail.

Intrinsic blood vessels

Vital microscopy has earlier been employed to determine critical levels for compression-induced occlusion of blood vessels in tracheal mucosa (Stenqvist & Bagge 1979), and in n. tibialis in rabbits (i.e., peripheral nerve; Rydevik et al. 1981). In both studies the pressure required to stop the arterial blood flow was close to the mean arterial blood pressure, which is in agreement with the findings in the present investigation. In the study on n. tibialis in rabbits, however, the authors choose another form of evaluation than in this study (Rydevik et al. 1981). Instead of calculating occlusion pressures, they described the microcirculatory events at each pressure level examined. This showed that the blood flow was stopped at 60–80 mm Hg in the arterioles, at 50–80 mm Hg in the capillaries, and at 40–60 mm Hg in the venules. The mean arterial blood pressure in this study was 78 mm Hg. There was thus an apparent difference in the distribution of occlusion pressures on the venular side between the results on peripheral nerves and the results on spinal nerve roots. According to figure 12, the nerve root venules were occluded by pressures in the range of 5-60 mm Hg. There is thus a population of venules that was occluded at pressures much lower than were seen in peripheral nerves. In fact some venules were found to be occluded at 5–10 mm Hg. However, there were venules that did not become occluded until the cauda equina was exposed to compression at 60 mm Hg. This suggests that the intrinsic venules may have an uneven exposure to applied mechanical deformation. The cauda equina is not a homogenous structure. It is formed by a number of independent nerve roots. If a vessel is located in the groove formed by two nerve roots the superficial tissues need to be displaced before such a vessel would be exposed to the balloon pressure. It may therefore be more protected from mechanical deformation than if it was located on the surface of a nerve root or outside the spinal dura in the epidural fat. It is also evident that a venule that is located between two arterioles may not be occluded until the arteriles are more or less occluded. The finding that some venules were not occluded until high pressures were applied may thus probably be explained by the anatomical location of the vessels.

Athough the venules may be occluded at pressures of 5–60 mm Hg, the results do not indicate how blood flow might be affected at pressure levels below the occlusion pressure. Probably there is significant impairment of the blood flow already at pressure levels far below the occlusion pressure as well. Such an incomplete impairment of blood flow was indicated in a recent study on the same model as used in the present investigation (Olmarker et al. 1991c). The results showed that complete restoration of venular blood flow, during stepwize deflation of the compression balloon, was not achieved until the compression was ended (i.e., 0 mm Hg).

The flow in the capillaries was found to be dependant upon the venular flow. If the flow in the venules is impaired, there may be a reduced flow in the connected capillaries. This "retrograde stasis" has been suggested to be an important mechanism for the development of symptoms in the carpal tunnel syndrome (Sunderland 1976). Due to the less developed venular network (Parke & Watanbe 1985), capillaries in the nerve root may thus be more affected by venular stasis than the capillaries in peripheral nerves. Since the results indicated that venular occlusion pressure is lower in nerve roots than in peripheral nerves, retrograde stasis might affect the nerve root capillaries at lower pressure levels than in peripheral nerves.

Nutritional supply

Methyl glucose is an uncharged and relatively small molecule. The transport mechanisms of methyl glucose are therefore similar to those of glucose and oxygen. Unlike these two nutrients, however, methyl glucose is a non-metabolizing solute, which makes it particularly suitable for studies on transport mechanisms of small solutes (Urban et al. 1978).

The R/Rco-ratio is a measurement of the concentration of methyl glucose in the tissue of the cauda equina (Olmarker et al. 1990a). Since the circulation time was fixed at five minutes, the R/Rco-ratio reflects the equilibration of the nerve root tissue to the blood concentration of methyl glucose during these five minutes. It is therefore also a measurement of the rate of transport of methyl glucose to the nerve roots. If enough time had been allowed there would have been an almost complete equilibration of the nerve root tissue, (i.e., a R/Rco-ratio close to 100%), even if the

transport of methyl glucose to the nerve roots had been impaired. It was therefore important to choose a circulation time that would both allow a high R/Rco-ratio in control experiments and at the same time being short enough to reveal any impairment of the transport of methyl glucose.

Nutrients are transported to the axons of the cauda equina both by the intrinsic vessels and by diffusion from the surrounding cerebrospinal fluid (Rydevik et al. 1990a). The cerebrospinal fluid pressure in pigs is about 8-11 mm Hg (Mount & Ingram 1971). When the cauda equina is exposed to pressures of 5–10 mm Hg, which is known to induce venular congestion in the most compression susceptible venules (Olmarker et al. 1989a), there is thus probably a certain amount of cerebrospinal fluid present around the nerve roots. Since diffusion from the cerebrospinal fluid is an important nutritional pathway for the nerve roots (Rydevik et al. 1990a), one may speculate that such diffusion might compensate for venular congestion with subsequent retrograde stasis of capillary networks. However, the results on the total nutritional transport to the nerve roots (Olmarker et al. 1990a), demonstrated that there were significant effects on the nutrition even at these low pressure levels. In fact, there was a statistically significant reduction of the nutritional transport, as compared to control, when only the balloon and plexiglass plate were placed on top of the cauda equina. Since compression-induced effects on the nutritional supply to the nerve roots were present even at this extremely low pressure level, it seems that diffusion from the cerebrospinal fluid can not completely compensate for compression-induced effects on the blood flow in the intrinsic vessels. Compression-induced effects of either of the two transport mechanisms can not be separated using the present experimental model. The observed reduction of the nutritional transport during sham-compression can therefore not specifically be contributed to either of them. The observed effect might be based on congestion of superficially located venules, and that diffusion from the cerebrospinal fluid may not have time to compensate for this loss during the 5 minutes of methyl glucose circulation time. However, although the mechanism is not clear, the study clearly demonstrates that there may be impairment of the nutritional transport present even at extremely low pressure levels, particularly since the reduction was so clearly located to the "compression zone" (Figure 13). The possible significance for nerve root nutrition and function, acute and long-term, remains to be elucidated.

There was a striking difference in the levels of methyl-glucose also outside the compression-zone between the rapid and the slow onset of compression at corresponding pressure levels. The R/Rco-graphs at the slow onset rate approached the control graph more rapidly than at the rapid onset rate. This observation may be important for understanding the pathophysiologic mechanisms behind the differences in effects, seen between the two onset rates employed in the present study. The possible mechanisms for this effect will be discussed below in the paragraph "rapid vs slow compression".

The R/Rco-graphs at the slow onset rate also suggested that the baselines outside the compression zone were dependant on the applied pressure. This may be an effect of stasis of the intrinsic vasculature at locations relativelly far from the compression zone, due to an impaired blood flow through the compressed nerve segment. The present study only comprized analyses of nerve root tissue up to 7 mm outside the compression zone. It is therefore unclear how far from the compression zone this effect was present. This difference between baselines at various compression pressure levels may also be the result of, for instance, vascular constriction outside the compressed segment due to metabolic or neurologic factors.

Intraneural edema formation

The effects of experimental compression on intraneural edema formation in peripheral nerves have been studied previously, using similar techniques for compression and evaluation as those in the present study (Rydevik & Lundborg 1977). These authors found that an endoneurial edema was induced following compression at either 50 mm Hg for 4–6 hours or 200 mm Hg for 2 hours. The onset rate was not presented, but has been estimated to 3–5 seconds by the authors. It was thus somewhere between the two onset rates used in the present study. The results of the present study thus indicate that the endoneurial capillaries of nerve roots seem to be more susceptible to compression injury than the corresponding vessels of peripheral nerves (Olmarker et al. 1989b).

In the same paper (Rydevik & Lundborg 1977), the effects of compression on the permeability of epineurial vessels was found to be similar to those in this study. The epineurial vessels of the peripheral nerves are not protected by the perineurium. This may make them anatomically more comparable to the endoneurial capillaries in the nerve roots. These data suggest that the difference in susceptibility to compression injury between endoneurial capillaries in peripheral nerves and nerve roots may be based on the presence of the perineurium in the peripheral nerves.

Intraneural edema is formed due to an increase in microvascular permeability of the endoneurial capillaries (Lundborg 1975, Rydevik & Lundborg 1977). This results in a leakage of fluid and macromolecules from these vessels out into the endoneurial space, which may negatively influence the nutrition of the nerve tissue by separating the axons and by altering the ionic balance within the endoneurium. Increasing amounts of fluid in the endoneurial space might also induce an increase in the endoneurial fluid pressure (Low & Dyck 1977, Myers & Powell 1981), particularly at locations where the nerve roots are enclosed by rigid structures, as for instance at the level of the intervertebral foramen. This may result in an subsequent impairment of the microcirculation within the endoneurium. An intraneural edema might thus result in a "compartment syndrome" within the peripheral nerve or the nerve root (Lundborg et al. 1983, Rydevik et al. 1989a), which may impair the nutritional supply (Low et al. 1982, Myers et al. 1982) and thus the function of the nerve roots.

Compression may induce edema formation in peripheral nerve tissue (Rydevik & Lundborg 1977), and dorsal root gangliae (Rydevik et al. 1989a). According to the present investigation (Olmarker et al. 1989b), such edema may be more easily induced in the cauda equina than in peripheral nerves (Rydevik & Lundborg 1977). An intraneural edema was also noted in by vital microscopy (Olmarker et al. 1989a). However, the pressure/time thresholds for occurrence of such edema was higher than observed in this study. This difference was most probably due to the higher sensitivity of the dye-tracing technique, employed in this study. An intraneural edema, as judged by vital microscopy, may be difficult to detect, since this distinction is based upon increasing opacity of the nerve roots and difficulties in focusing on the borders of the intraneural vessels.

Intraneural edema may be formed as the result of ischemia. The blood-nerve barrier of peripheral nerves has been shown to be impaired, with a subsequent edema formation, when exposed to ischemia for 8 hours or more (Lundborg 1970). However, if compression was added, edema formation was observed after 2–4 hours (Lundborg 1970). The combination of compression and ischemia is thus more deleterious than ischemia alone regarding the integrity of the blood-nerve barrier in peripheral nerves.

Edema was found to be most pronounced at the edges of the compressed cauda equina segment. This is in agreement with previous observations in compressed peripheral nerves (Rydevik & Lundborg 1977). The mechanism for this phenomenon may be related to a displacement of the compressed nerve tissue (Rydevik et al. 1984, 1989b). When a nerve is compressed, there is a displacement of the compressed nerve tissue towards the uncompressed parts of the nerve (Ochoa et al. 1972, MacGregor et al. 1975). The superficial parts of the nerve are displaced more than the deeper parts. Shearing may thus occur between the different layers of the displaced nerve, which are maximized at the edge zones (Rydevik et al. 1984). This shearing would be particularly injurious to the blood vessels which run obliquely in the endoneurial space.

Due to the less developed blood-nerve barrier of the endoneurial capillaries, a compression-induced edema has been suggested to be formed more easily in nerve roots than in peripheral nerves (Rydevik et al. 1984). This suggestion was supported by the results of the present investigation (Olmarker et al. 1989b). Another factor for the development of an intraneural edema that has been suggested is the release of "heparin and biogenic amines" from endoneurial mast cells (Lundborg 1975). However, unlike in peripheral nerves, there are no mast cells present in the endoneurium of the spinal nerve roots (Gamble 1964).

Although more easily induced in nerve roots, intraneural edema is probably more deleterious to the peripheral nerves, once formed. In a peripheral nerve, each nerve fascicle is surrounded by the perineurium. The perineurium constitutes an efficient diffusion barrier for fluid and macromolecules (Olsson & Reese 1969, 1971b, Klemm 1970, Rydevik & Lundborg 1977). An edema will therefore be "trapped" within the perineurium. The spinal nerve roots do not possess a similar diffusion barrier. An endoneurial edema will therefore more easily be drained out into the surrounding cerebrospinal fluid. However, at locations where the meninges enclose the nerve roots tightly, such as the intervertebral foramen, an edema may be more deleterious. Since the dorsal root ganglion is enclosed with a strong meningeal capsule, this location could also be particularly susceptible to the effects of an intraneural edema (Rydevik et al. 1989a).

Intraneural edema is probably a common feature in nerve root compression lesions. The presence of edema in compressed lumbosacral nerve roots has been observed both with CT-scans (Takata et al. 1988) and in histologic sections of nerve roots at cadaveric studies (Hoyland et al. 1988). Even if compressed lumbosacral nerve roots are decompressed surgically, it would probably take some time for edema to be eliminated from the endoneurial space. The presence of edema may thus impair the nutrition of the nerve roots for longer periods of time than the compression itself. A longstanding edema may also be related to the formation of an intraneural fibrotic scar (Lundborg 1975, Rydevik et al. 1976). Formation of an intraneural

edema, with or without fibrosis, might thus contribute to the slow recovery observed in some patients with nerve root compression syndromes.

Effects on nutrition vs impulse propagation

Other experiments with cauda equina compression in the pig, using similar neurophysiologic analyses as in this study, gave results which were similar to those obtained with the slow onset rate (Pedowitz et al. 91, Rydevik et al. 1991a). The onset rate employed in those studies were 3–5 seconds, (i.e., between the two onset rates employed in the present study).

Similar studies on a peripheral nerve, (n. tibialis, rabbit), have demonstrated a 30% decrease of the initial action potential after compression for 2 hours at 50 mm Hg (Rydevik & Nordborg 1980). The onset rate was not presented, but estimated to 3–5 seconds by the authors. The effects on n. tibialis were thus slightly more pronounced than the effects on the cauda equina seen in this study. Dahlin and collaborators recently reported that impulse propagation in n. peroneus communis in rabbits, compressed with the same compression device as used by Rydevik and Nordborg for n. tibialis, was more impaired than n. tibialis at corresponding pressures (Dahlin et al. 1989). Compression at 200 mm Hg in n. tibialis resulted in a 85% decrease of the initial amplitude after 2 hours (Rydevik & Nordborg 1980), and in n. peroneus communis in a complete conduction block after 23 minutes (Dahlin et al. 1989). It was suggested that this difference was based on differences in amounts of surrounding connective tissue sheaths between the two nerves (Dahlin et al. 1989). These results thus indicate that there can be differences in compression susceptibility even between adjacent nerves in the same species. This also means that it may be difficult to make any general statements of differences in compression-induced impairment of impulse propagation between peripheral nerves and spinal nerve roots.

It was recently demonstrated that 50 mm Hg compression of spinal nerve roots using the present compression model, did not significantly impair impulse propagation during a 2 hour compression period (Pedowitz et al. 1991, Rydevik et al. 1991a) and only minor changes were observed during a 4 hour compression period (Pedowitz et al. 1989). This is in agreement with the present results. The effects of compression on impulse propagation might thus seem contradictory to the results on the nutritional transport, which showed a marked reduction of the nutritional transport at 50 mm Hg at both onset rates. However, there might probably be a delay before a nutritional impairment may lead to changes in nerve conduction properties. A significant impairment of the nutritional transport mechanisms may be injurious to the normal function of the nerve roots during prolonged compression periods. In various clinical situations, the compression periods are more likely to last for days or months rather than for minutes or hours. The results on intraneural blood flow (Olmarker et al. 1989a) and on the nutritional transport (Olmarker et al. 1990a) indicate that a significant impairment of the nutritional transport may be induced at 10–50 mm Hg. This suggests that neural dysfunction could be induced, even by low compression pressures, in nerve root compression syndromes.

Similar to the studies on nutritional transport (Olmarker et al. 1990a) and edema formation (Olmarker et al. 1989b), there was a significant difference in effects between the two compression onset rates employed. The mechanisms involved will be discussed below in the paragraph "rapid vs slow onset of compression".

Rapid vs slow onset of compression

The present investigation demonstrated that a rapid compression onset rate (0.05–0.1 sec.) induced more pronounced effects than a slower onset rate (20 sec.) on nutritional transport (Olmarker et al. 1990a), vascular permeability (Olmarker et al. 1989b), and impulse propagation (Olmarker et al. 1990b) in the spinal nerve roots. On-going studies has also shown that compression at 600 mm Hg for 2 seconds is sufficient to induce a progressive impairment of nerve conduction if compression is applied with the rapid onset rate (Olmarker et al. 1991d)

The first question that arises is if this observed difference may be based on differences in compression exposure, (i.e., compression level x compression duration). During the slow onset, the compression was not 100% of the intended value until 20 seconds after initiating the compression. The nerve roots subjected to the rapid onset rate were thus exposed to a higher compression exposure. However, the compression exposure ratio between slow and rapid onset rates are 92% at compression for 2 minutes, 98.4% at 10 minutes and 99.9% at 2 hour compression. These differences thus seem too small to be solely responsible for the pronounced differences seen in the present investigation. Other mechanisms may therefore probably be found in the initial reaction pattern of the nerve tissue to the applied compression.

Nerve compression induces mechanical deformation of the nerve tissue and also effects on the nutritional supply to the nerve tissue (Dahlin et al. 1986). According to the effects of compression on impulse propagation (Olmarker et al. 1990b), there was no difference in reduction of muscle action potential between the two onset rates during the first minute of compression (Figure 15). This implies that there are probably no severe mechanical effects, such as axonal breakage, induced early in the compression onset. However, since there is a difference visible after 2–5 minutes, any potential mechanisms are probably present early in the compression period, most probably during the compression onset. The results on nerve impulse propagation (Olmarker et al. 1990b) also indicate that the effects are progressive, since the MAP-amplitudes decreased with time.

Nerve tissue has visco-elastic properties (Rydevik et al. 1989b, 1991b). This implies that the rate of mechanical deformation is of a certain importance for the injury pattern. The energy that is imposed on the nerve tissue during compression is probably equivalent between the two onset rates. However, at the rapid onset rate, the energy is transferred to the nerve tissue during a shorter period of time than at the slow onset rate. This implies that the energy per time unit transferred to the nerve tissue is higher at the rapid onset rate, a theory that might serve as one general explanation for the observed differences between the two onset rates.

If the energy that is transferred from the compression balloon to the nerve tissue can not be absorbed as movement or heat, there will be plastic deformation, (i.e., irreversible mechanical deformation), of the compressed tissue. This would probably result in structural changes, even at the sub-cellular level. However, although such a mechanism might be present, there is in fact a movement of the nerve tissue from the compressed to the uncompressed parts of the nerve roots (Ochoa et al. 1972, MacGregor et al. 1975). This displacement of nerve tissue may suggests one possible theory for the observed difference between rapid and slow onset rates, that might also be supported by results from the present investigation.

An arbitrary point (A) is displaced from its initial position (A_o) to the position at equilibrium (A_e) during compression, (Figure 16). The distance A_o–A_e is dependant on the magnitude of the applied compression pressure and on the biomechanical properties of the nerve tissue. The rate at which the point A is displaced is dependant on the onset rate of the applied compression. If the compression is applied slowly, there will be a slow displacement of A towards A_e. If the compression onset rate is increased, the displacement rate will increase accordingly. However, at a certain threshold of onset rate, A may be displaced slightly further than to A_e, which means that there will be an "over-displacement" of A before it will rebound towards A_e (Figure 16). With increasing onset rates, this over-displacement will increase. A rapid compression onset rate would thus induce a higher over-displacement than a slower onset rate. Although probably not present more than during fractions of seconds, this over-displacement might induce local mechanical deformation that might negatively influence the normal nutrition and function of the spinal nerve roots.

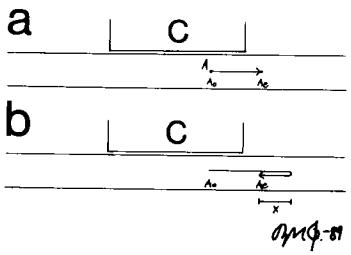

Figure 16. When compression is applied gradually (a), there will be a slow displacement of an arbitrary point (A) from its initial position (A_o) to its position at equilibrium (A_e) during compression. If the compression is applied rapidly (b), A may be displaced slightly further before rebounding to A_e. There will thus an "over-displacement" of A (x) before reaching equilibrium during compression. (Reproduced with permission from, Olmarker K, Thesis, Gothenburg 1990).

It has been observed that compression-induced effects on peripheral nerves are most pronounced at the edges of the compression zone (Bentley & Schlapp 1943, Edwards & Cattell 1928, Ochoa et al. 1972, Rydevik & Lundborg 1977). It has been suggested that this so called "edge-effect" is due to a displacement of the compressed nerve tissue towards the uncompressed parts of the nerve. Mathematical models have indicated that the displacement is maximal at the edges of the compressed segment, and also that the superficial parts of the nerve are displaced more than the deeper parts (Rydevik et al. 1984, 1989b). During displacement, occurs between the different layers of the nerve. A structure passing obliquely through the nerve tissue might therefore be more susceptible to injury induced by the displacement. This would suggest that endoneurial capillaries would be more at risk, than longitudinally running nerve fibers, of being injured by the induced shear-strain. The injury pattern for the nerve fibers with paranodal invagination (Ochoa et al. 1972, Rydevik & Nordborg 1980) is compatible with deformation due to the longitudinal displacement per se in a given layer of the nerve or nerve root (Rydevik et al. 1989b).

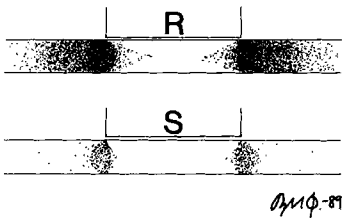

Figure 17. Drawing illustrating the hypothesis that a more pronounced edema might affect a wider nerve root segment than a less pronounced edema. The edema induced by a rapid onset rate (top) is more pronounced than for a slow onset rate (bottom). The former may thus affect a longer segment of the nerve roots. (Reproduced with permission from, Olmarker K, Thesis, Gothenburg 1990).

The rapid onset rate was found to increase the microvascular permeability more than the slow onset (Olmarker et al. 1989b). The edema that was formed due to this increase in permeability was most pronounced at the edge-zones. This suggests that the displacement might be of importance for the increase in vascular permeability. If the difference in microvascular permeability should be based on differences in over-displacement induced by the two compression onset rates, the injury would have been induced early in the compression onset. This would result in a vascular injury with subsequent progressive edema formation developing in the nerve. This mechanism may thus relate to the progressive impairment of impulse propagation observed (Olmarker et al. 1990b). An edema would probably not be formed only within the compression zone. Instead it would be formed mainly in the uncompressed parts of the nerve roots, adjacent to the compression zone. In such a way, it could thus interfere with the nutritional transport to both the compressed and the uncompressed parts adjacent to the compression zone of the nerve roots. The degree of edema would therefore also relate to the width of the nutritionally impaired nerve root segment (Figure 17). The zone of impaired nutritional transport outside the compression zone may also relate to the differences in R/Rco-ratios outside the compression zone between the rapid and the slow onset rate observed for the nutritional transport (Figure 13; Olmarker et al. 1990a) as well as within the compression zone, due to an impairment of the nutritional transport into the compressed segment. The hypothesis that the width of the compressed segment is of importance for the magnitude of compresion-induced effects is partly supported by on-going studies in which two balloons are placed over the cauda equina. Preliminary results show that 10 mm Hg is sufficient to induce a significant impairment of MAP-amplitude when two balloons are placed 10 mm apart (Olmarker et al. 1991b). Due to the vascular anatomic arrangment, with no regional arteriolar blood supply, the blood flow in the nerve segment between two compression sites should be affected as well. This has also been confirmed by recent studies (Cornefjord et al. 1991, Takahashi et al. 1991a, 1991b).

Grundfest observed in in vitro experiments that a nerve that is subjected to high pressures in a pressure chamber is relatively resistant to compression regarding impulse propagation as long as adequate concentrations of oxygen are present (Grundfest 1936). However, at comparatively low pressure levels, local compression can block impulse conduction (Bentley & Schlapp 1943, Rydevik & Nordborg 1980). These data have stressed the importance of the pressure gradient between compressed and uncompressed nerve tissue. It is possible that pressure distribution at the compression site may vary between the two onset rates, and that this may contribute to the observed differences.

Another possible mechanism that might be responsible for the difference in effects between the two onset rates is a trapping phenomenon of blood within the compression zone. Blood was often seen macroscopically in the vessels within the compression zone in nerve roots exposed to the rapid onset rate. This was not observed at the slow onset rate. It thus seems that the vessels might have been occluded at the edge zones by the displacement, when exposed to the rapid onset rate (Lauritzen et al. 1981). The blood was thus "trapped" within the compression zone. However, when applying pressure at the slow onset rate, the blood might have been able to leave the compressed segment. Trapped leucocytes may leak agents such as toxic oxygen compounds, proteolytic enzymes and longacting oxidants, which may damage the endothelial cells of the endoneurial capillaries (Ernst et al. 1987). These substances may impair the normal barrier function of the capillaries, which thus may lead to edema formation. Such mechanisms may be initiated when the blood cells are in contact with oxygenated blood. The most critical phase, with respect to trapped blood cells, will therefore be the recirculation of a compressed nerve segment. However, trapped blood cells might probably also reach the edges of the compression zone with time. Since oxygenated blood may be present in the nerve tissue adjacent to the compression zone (Olmarker et al. 1990a), there is a possibility that any effects of substances from the formerly trapped blood cells may act at the edges of the compressed nerve segment. In such a way they might contribute to differences in edema formation between the two compression onset rates studied, which were most pronounced at this location (Olmarker et al. 1989b).

Summary and Conclusion

Summary

A model for experimental studies of acute, graded compression of the cauda equina in pigs was presented (Olmarker et al. 1991a). Detailed analyses of the neural and vascular anatomy demonstrated a close resemblance to the human cauda equina. There were structural and vascular differences between spinal nerve roots and peripheral nerves that could contribute to differences in compression susceptibility between these two parts of the nervous system. The pressure transmission from the balloon to the nerve roots showed to have a high accuracy.

The occlusion-pressures for the arterioles, capillaries and venules of the cauda equina were determined (Olmarker et al. 1989a). Arteriolar blood flow was stopped at a pressure close to the mean arterial blood pressure. Capillary blood flow was found to be dependent upon flow in the connected venules. The blood flow in some venules was found to be stopped at 5–10 mm Hg. However, venular occlusion pressures ranged from 5 to 60 mm Hg. Compression up to 200 mm Hg for 2 hours did not induce a "no-reflow" phenomenon when the compression was ended. However, a transient hyperemia was noted at all pressure/time relations studied, indicating nutritional deficit in the compressed segment during compression. Signs of edema were seen in nerve roots exposed to compression for 2 hours at either 50 or 200 mm Hg.

The nutritional supply to the cauda equina was found to be impaired at low pressure levels (less than 10 mm Hg; Olmarker et al. 1990a). Diffusion from adjacent tissues with a better nutritional supply, including the cerebrospinal fluid, could thus not compensate completely for compression-induced effects on the transport of nutrients. However, a certain nutritional supply to the compressed segment was present even at 200 mm Hg compression. There were more pronounced effects on the nutritional supply induced by a rapid (0.05–0.1 sec.) than a slow (20 sec.) compression onset rate. Nutritional impairment was noted both within and outside the compressed nerve segment.

An increase in vascular permeability was induced by compression at 50 mm Hg for 2 minutes (Olmarker et al. 1989b). The magnitude of this permeability increase was dependant on both the magnitude and the duration of compression. The permeability increase was more pronounced for the rapid than for the slow compression onset rate at all pressure/time relations studied.

Reduction of muscle action potential (MAP) amplitude in tail muscles, after stimulation cranial to the compression zone, was induced by compression at 100 and 200 mm Hg for 2 hours (Olmarker et al. 1990b). The reduction was more pronounced at 200 than 100 mm Hg. The recovery after compression was also slower at 200 than 100 mm Hg. Sham compression and compression at 50 mm Hg induce no or only minor reduction of MAP-amplitude. The reduction of MAP-amplitude was more pronounced for the rapid than for the slow compression onset rate, and was statistically significant at 100 and 200 mm Hg compression.

Conclusion

The spinal nerve roots are generally well protected from external trauma by the vertebrae. However, if subjected to a direct trauma the nerve roots may be severely affected, even at low pressure levels. The compression onset rate also seems to be of importance for the degree of compression-induced effects that might be acquired in various conditions resulting in nerve root compression.

The present investigation focused on the acute effects of nerve root compression in an experimental model. The pathogenetics in clinical nerve root compression conditions are of course much more complex. For instance, the presence of an intraneural edema may be related to fibroblast invasion and chronic impairment of axonal transport as well as intraneural microcirculation may induce changes that could not be assessed in a model for acute compression. Such a complex sequence of events could via various mechanisms lead to nerve root pain production and nerve dysfunction. However, although the present investigation was limited to acute changes in nerve root nutrition and function, it may serve as a basis for continued evaluation of pathogenetic mechanisms in both acute and chronic nerve root compression disorders.

Acknowledgements

This work was the result of cooperation between the Laboratory of Experimental Biology, Department of Anatomy, and the Department of Orthopedics, Sahlgren Hospital, both at the University of Göteborg.

I would like to express my sincere gratitude to:

Professor Per-Ingvar Brånemark, head of the Laboratory of Experimental Biology; Associate professor Björn Rydevik; Associate professor Sten Holm; Professor Alf Nachemson, chairman of the Department of Orthopedics; Dr. Robert Pedowitz, University of California San Diego, USA; Associate professor Ulf Bagge; Professor Tommy Hansson; Ms. Anna-Lena Rosenqvist; Professor Richard Skalak, University of California San Diego, USA; Professor Malcolm Pope, Vermont University, Burlington, USA; Professor Manohar Panjabi, Yale University, New Haven, USA; Assistant professor Nils Danielsen; Assistant professor Lars B. Dahlin; Mr. Erik Hult; Mr. Lars Ekström and family, friends and colleagues.

The investigations have been supported by grants from the Swedish Medical Research Council (8685, 9758), the Folksam Research Foundation, the Institute for Applied Biotechnology, Greta and Einar Asker's Research Foundation, the Carin Trygger Memorial Foundation, the Gothenburg Medical Society and the University of Göteborg.

References

Adamkiewicz A. Die Blutgefässe des menschlichen Rückenmarkes. I. Die Gefässe der Rückenmarkssubstanz. *Sitzungsb. d. k. Akad. d. Wissensch. in Wien. math.-naturw.* 84:469-502, 1881

Adamkiewicz A. Die Blutgefässe des menschlichen Rückenmarkes. II. Die Gefäse der Rückenmarksoberfläche. *Sitzungsb. d. k. Akad. d. Wissensch. in Wien math.-naturw.* 85:101-130, 1882

Adams HD, van Geertruyden HH. Neurolgic complications of aortic surgery. *Ann Surg* 144:574-610, 1956

Bentley FH, Schlapp W. The effects of pressure on conduction in peripheral nerve. *J Physiol* 72-82, 1943

Berthold CH, Carlstedt T, Corneliuson O. Chapter 6. Anatomy of the nerve root at the central-peripheral transitional region. In: *Peripheral Neuropathy,* vol 1. PJ Dyck, PK Thomas, EH Lambert, R Bunge (Eds). WB Saunders Company, Philadelphia, London, Toronto, Mexico City, Rio de Janerio, Sydney & Tokyo, pp 156-170, 1984

Clarke E, Bearn JG. The spiral nerve bands of Fontana. *Brain* 95:1-20, 1972

Cohen MS, Wall EJ, Brown RB, Garfin SR. Cauda equina anatomy. Part II: Extrathecal nerve roots and dorsal root ganglia. *Spine* (in press), 1991

Corbin JL. Anatome et pathologie arterielles de la moelle. Masson et Cie, Paris, 1961

Cornefjord M, Olmarker K, Takahashi K, Rydevik B, Holm S. Impairment of nutritional transport at double level cauda equina compression. Trans. International Society for the Study of the Lumbar Spine, Heidelberg, Germany, May 1991.

Crock HV, Yoshizawa H. The blood supply of the lumbar vertebral column. *Clin Orthop* 115:6-21, 1976

Dahlin LB, Rydevik B, Lundborg G. Pathophysiology of nerve entrapments and nerve compression injuries. In: *Tissue nutrition and viability.* Hargens AR (ed). Springer-Verlag, Berlin, Heidelberg, New York, pp135-160, 1986

Dahlin LB, Shyu BC, Danielsen N, Andersson SA. Effects of nerve compression or ischemia on conduction properties of myelinated and non-myelinated nerve fibres. An experimental study in the rabbit common peroneal nerve. *Acta Physiol Scand* 136:97-105, 1989

Desproges-Gotteron R. Contribution à l'étude de la sciatique paralysante. Thesis no 342, Paris, 1955

Dommisse GF. Arteries and veins of the lumbar nerve roots. *Clin Orthop* 115:22-29, 1976

Duret H. Note sur les artères nourricières et sur les vaisseaux capillaires de la moelle épinière. *Progr méd* 1:284, 1873a

Duret H. Conclusion d'un mémoire sur la circulation bulbaire. *Arch Physiol Norm et Path* 50:88-89, 1873b

Edwards DJ, Cattell MK. Further observations on decrement in nerve conduction. *Am J Physiol* 87:359-367, 1928

Ernst E, Hammerschmidt DE, Bagge U, Matrai A, Dormandy JA. Leukocytes and the risk of ischemic disease. *JAMA* 257:2318-2324, 1987

Fried LC, Doppman J. The arterial supply to the lumbo-sacral spinal cord in the monkey. A comparison with man. *Anat Rec* 178:41-48, 1958

Gamble HJ. Comparative electron-microscopic observations on the connective tissues of a peripheral nerve and a spinal nerve root. *J Anat* (Lond) 98:17-25, 1964

Gamble HJ, Eames RA. Electron microscopy of human spinal-nerve roots. *Arch Neurol* 14:50-53, 1966

Gasser HS, Erlanger J. The role of fiber size in the establishment of a nerve block by pressure and cocain. *Am J Physiol* 88:581-591, 1929

Gelfan S, Tarlov IM. Physiology of spinal cord, nerve root and peripheral nerve compression. *Am J Physiol* 185:217-229, 1956

Gillilan LA. The arterial blood supply of the human spinal cord. *J Comp Neurol* 110:75-103, 1958

Grundfest H. Effects of hydrostatic pressure upon the excitability, the recovery, and the potential sequence of frog nerve. *Cold Spring Harb Symp Quant Biol* 4:179-187, 1936

Haller FR, Low FN. The fine structure of the peripheral nerve root sheath in the subarachnoid space in the rat and other laboratory animals. *Am J Anat* 131:1-20, 1971

Herren RY, Alexander L. Sulcal and intrinsic blood vessels of human spinal cord. *Arch Neurol Psychiat* 41:678-687, 1939

Hoyland JA, Freemont AJ, Jayson MIV. Peri-radicular vascular changes in relation to disc prolapse and osteophytosis. Trans. the International Society for the Study of the Lumbar Spine, Miami, Florida, April, 1988

Kadyi H. Über die Blutgefässe des menschlichen Rückenmarkes. *Anat Anz* 1:304-314, 1886 (Cited by Gillilan 1958)

Klemm H. Das Perineurium als Diffusionsbarriere gegenüber Peroxydase bei epi- und endoneuraler Applikation. *Z Zellforsch* 108:431-445, 1970

Lauritzen C, Bagge U, Romanus M. The effects of pressure and its duration on microcirculation and healing of skin flaps. An experimental study in rabbits. *Scand J Plast Reconstr Surg* 15:5-8, 1981

Lazorthes G, Gouazé A, Bastide G, Soutoul J-H, Zadeh O, Santini J-J. La vascularisation artérielle du renflement lombaire. Étude des variations et des suppléances. *Rev Neurol* 114:109-122, 1966

Lazorthes G, Gouaze A, Zadeh JO, Santini JJ, Lazorthes Y, Burdin P. Arterial vascularization of the spinal cord. Recent studies of the anastomtic substitution pathways. *J Neurosurg* 35:253-262, 1971

Low PA, Dyck PJ. Increased endoneurial fluid pressure in experimental lead neuropathy. *Nature* 269:427-428, 1977

Low PA, Dyck PJ, Schmelzer JD. Chronic elevation of endoneurial fluid pressure is associated with low-grade fiber pathology. *Muscle Nerve* 5:162-165, 1982

Lundborg G. Ischemic nerve injury. Experimental studies on intraneural microvascular pathophysiology and nerve function in a limb subjected to temporary circulatory arrest. *Scand J Plast Reconstr Surg* (Suppl 16), 1970

Lundborg G. Structure and function of the intraneural microvessels as related to trauma, edema and nerve function. *J Bone Joint Surg* 57A: 938-948, 1975

Lundborg G, Myers R, Powell H. Nerve compression injury and increased endoneurial fluid pressure: a "miniature compartment syndrome". *J Neurol Neurosurg Psychiat* 46:1119-1124, 1983

MacGregor RJ, Sharpless SK, Luttges MW. A pressure vessel model for nerve compression. *J Neurol Sci* 24:299-304, 1975

McCabe JS, Low FN. The sub-arachnoid triangle: An area of transition in peripheral nerve. *Anat Rec* 164:15-34, 1969

Mount LE, Ingram DL. The pig as a laboratory animal. Academic Press, London, New York, 1971

Murphy RW. Nerve roots and spinal nerves in degenerative disk disease. *Clin Orthop* 129:46-60, 1977

Myers RR, Powell HC. Endoneurial fluid pressure in perpiheral neuropthies, Tissue fluid pressure and composition, Ed AR Hargens, Baltimore, Williams & Wilkins, pp 193-207, 1981

Myers RR, Mizisin AP, Powell HC, Lampert PW. Reduced nerve blood flow in hexachlorophene neuropathy. Relationship to elevated endoneurial fluid pressure. *J Neuropathol Exp Neurol* 41:391-399, 1982

Nachemson AL, Andersson GBJ. Classification of low back pain. *Scand J Work Environ Health* 8:134-136, 1982

Ochoa J, Fowler TJ, Gilliat RW. Anatomical changes in peripheral nerves compressed by a pneumatic tourniquet. *J Anat* 113:433-455, 1972

Olmarker K, Rydevik B, Holm S, Bagge U. Effects of experimental, graded compression on blood flow in spinal nerve roots. A vital microscopic study on the porcine cauda equina. *J Orthop Res* 7:817-823, 1989a

Olmarker K, Rydevik B, Holm S. Edema formation in spinal nerve roots induced by experimental, graded compression. An experimental study on the pig cauda equina with special reference to differences in effects between rapid and slow onset of compression. *Spine* 14:569-573, 1989b

Olmarker K, Rydevik B, Hansson T, Holm S. Compression-induced changes of the nutritional supply to the porcine cauda equina. *J Spinal Dis* 3:25-29, 1990a

Olmarker K, Holm S, Rydevik B. Importance of compression onset rate for the degree of impairment of impulse propagation in experimental compression of the porcine cauda equina. *Spine* 15:416-419, 1990b

Olmarker K, Holm S, Rosenqvist A-L, Rydevik B. Experimental nerve root compression. Presentation of a model for acute, graded compression of the porcine cauda equina, with analyses of neural and vascular anatomy. *Spine* 16:61-69, 1991a

Olmarker K, Holm S, Rydevik. Single versus double level nerve root compression. An experimental study on the porcine cauda equina with analyses of nerve impulse conduction properties. Symposium on "Newest knowledge on Low back pain", invited paper. *Clin Orthop* (in press), 1991b

Olmarker K, Holm S, Rydevik B, Bagge U. Restoration of intrinsic blood flow during gradual decompression of the porcine cauda equina. A vital microscopic study. *Neuro-orthop* 10:83-87, 1991c

Olmarker K, Lind B, Holm S, Rydevik B. Continued compression increases impairment of impulse conduction in experimental compression of the porcine cauda equina. *Neuroorthop* (In press), 1991d

Olsson Y, Reese TS. Inaccessibility of the endoneurium of mouse sciatic nerve to exogenous proteins. American association of anatomists' 82nd Annual session. *Anat Rec* 163:138, 1969

Olsson Y, Reese TS. Permeability of vasa nervorum and perineurium in mouse sciatic nerve studied by fluorescence and electronmicroscopy. *J Neuropathol Exp Neurol* 30:105-119, 1971b

Parke WW, Gamell K, Rothman RH. Arterial vascularization of the cauda equina. *J Bone Joint Surg* 63A:53-62, 1981

Parke WW, Watanabe R. The intrinsic vasculature of the lumbosacral spinal nerve roots. *Spine* 10:508-515, 1985

Pedowitz RA, Garfin SR, Hargens AR, Swenson MR, Myers RR, Massie JB, Rydevik BL. Effects of magnitude and duration of compression on spinal nerve root conduction. *Spine* (in press) 1991

Petterson CÅV, Olsson Y. Blood supply of spinal nerve roots. An experimental study in the rat. *Acta Neuropathol* 78:455-461, 1989

Rauschning W. Computed tomography and cryomicrotomy of lumbar spine specimens. A new technique for multiplanar anatomic correlation. *Spine* 8:170-180, 1983

Rauschning W. Normal and pathologic anatomy of the lumbar root canals. *Spine* 12:1008-1019, 1987

Richardsson KC, Jarett L, Finke EH. Embedding in epoxy resins for ultrathin sectioning in electron microscope. *Stain Technol* 35:313-323, 1960.

Rydevik B, Lundborg G, Nordborg C. Intraneural tissue reactions induced by internal neurolysis. *Scand J Plast Reconstr Surg* 10:3-8, 1976

Rydevik B, Lundborg G. Permeability of intraneural microvessels and perineurium following acute, graded nerve compression. *Scand J Plast Reconstr Surg* 11:179-187, 1977

Rydevik B, Nordborg C. Changes in nerve function and nerve fiber structure induced by acute, graded compression. *J Neurol Neurosurg Psychiatry* 43:1070-1082, 1980

Rydevik B, Lundborg G, Bagge U. Effects of graded compression on intraneural blood flow. *J Hand Surg* 6:3-12, 1981

Rydevik B, Brown MD, Lundborg G. Pathoanatomy and pathophysiology of nerve root compression. *Spine* 9:7-15, 1984

Rydevik B, Myers RR, Powell HC. Pressure increase in the dorsal root ganglion following mechanical compression. Closed compartment syndrome in nerve roots. *Spine* 14:574-576, 1989a

Rydevik B, Lundborg G, Skalak R. Biomechanics of peripheral nerves. In: *Basic biomechanics of the musculoskeletal system.* M Nordin, VH Frankel (Eds). Lea and Febiger, Philadelphia, pp 75-87, 1989b

Rydevik B, Holm S, Brown MD, Lundborg G. Diffusion from the cerebrospinal fluid as a nutritional pathway for spinal nerve roots. *Acta Physiol Scand* 138:247-248, 1990a

Rydevik BL, Kwan MK, Myers RR, Brown RA, Triggs KJ, Woo S L-Y, Garfin SR. An in vitro mechanical and histological study of acute stretching on rabbit tibial nerve. *J Orthop Res* 8:694-701, 1990b

Rydevik BL, Pedowitz RA, Hargens AR, Swenson MR, Myers RR, Garfin SR. Effects of acute graded compression on spinal nerve root function and structure: An experimental study on the pig cauda equina. *Spine* 16:487-493, 1991

Sharpless SK. Susceptibility of spinal nerve roots to compression block. The research status of spinal manipulative therapy. NIH-workshop, February 2-4 1975. NINCDS Monograph no.15, edited by M Goldstein, pp 155-161, 1975

Steer JM. Some observations on the fine structure of rat dorsal spinal nerve roots. *J Anat* 109:467-485, 1971

Stenqvist O, Bagge U. Cuff pressure and microvascular occlusion in the tracheal mucosa. *Acta Otolaryngol* 88:451-454, 1979

Stodieck LS, Beel JA, Luttges MW. Structural properties of spinal nerve roots: Protein composition. *Exp Neurol* 91:41-51, 1986

Suh TH, Alexander L. Vascular system of the human spinal cord. *Arch Neurol Psychiat* 41:659-677, 1939

Sunderland S. The nerve lesion in the carpal tunnel syndrome. *J Neurol Neurosurg Psychiatry* 39:615-626, 1976

Sunderland S. Nerves and nerve injuries. 2nd edition. Churchill, Livingstone, Edinburgh, 1978

Takahashi K, Olmarker K, Rydevik B, Holm S. Analyses of intraneural blood flow at double level cauda equina compression in the pig. Trans. Orthopaedic Research Society, Anaheim, USA, March 1991a

Takahashi K, Olmarker K, Rydevik B, Holm S. Continuous monitoring of intraneural blood flow. Trans. International Society for the Study of the Lumbar Spine, Heidelberg, Germany, May 1991b

Takata K, Inoue S-I, Takahashi K, Ohtsuka Y. Swelling of the cauda equina in patients who have herniation of a lumbar disc. *J Bone Joint Surg* 70A: 361-368, 1988

Tanon L. Les artères de la moelle dorsolombaire. Thesis, Paris 1908

Tarlov IM. Structure of the nerve root. I Nature of the junction between the central and the peripheral nervous system. *Arch Neurol Psyciat* 37:555-583, 1937

Thomas PK, Olsson Y. Chapter 4. Microscopic anatomy and function of the connective tissue components of peripheral nerve. In: *Peripheral Neuropathy,* vol 1. PJ Dyck, PK Thomas, EH Lambert, R Bunge (Eds). WB Saunders Company, Philadelphia, London, Toronto, Mexico City, Rio de Janerio, Sydney, Tokyo, pp 97-120, 1984

Thomsen R. Über eigenthümlige aus veränderten Ganglienzellen hervorgegangene Gebilde in den Stämmen der Hirnnerven des menschen. *Virschovs Arch f Path Anat* 109:459, 1887

Urban JPG, Holm S, Maroudas A. Diffusion of small solutes into the intervertebral disc: An in vivo study. *Biorheology* 15:203-223, 1978

Waggener JD, Beggs J. The membranous coverings of neural tissues: An electron microscopy study. *J Neuropath* 26:412-426, 1967

Wall EJ, Cohen MS, Massie JM, Rydevik B, Garfin SR. Cauda equina anatomy. Part I: Intrathecal nerve root organisation. *Spine* (in press), 1991

Viraswami V. A study of the blood supply of the nerve roots in man and the rabbit with an experimental analysis of the collateral circulation following ligature of the arteries. Thesis, London, 1963